JOURNAL OF GEOPHYSICAL RESEARCH, VOL. 98, NO. A7, PAGES 11,319–11,337, JULY 1, 1993

Structure and Properties of the Subsolar Magnetopause for Northward Interplanetary Magnetic Field: Multiple-Instrument Particle Observations

P. SONG,[1,2] C. T. RUSSELL,[1] R. J. FITZENREITER,[3] J. T. GOSLING,[4] M. F. THOMSEN,[4]
D. G. MITCHELL,[5] S. A. FUSELIER,[6] G. K. PARKS,[7]
R. R. ANDERSON,[8] AND D. HUBERT[9]

The structure and properties of the subsolar magnetopause for northward interplanetary magnetic feild (IMF) are studied with measurements from 10 different instruments for three ISEE crossings. Data show that the overall structure and properties are similar for the three crossings, indicating the magnetopause is relatively well determined in the subsolar region for strongly northward IMF. The measurements from different instruments are consistent with each other and complementary based on the current knowledge of space plasma physics. The combined data set suggests that the magnetopause region is best organized by defining a sheath transition layer and steplike boundary layers. The sheath transition layer contains mostly magnetosheath particles. The magnetosheath, magnetospheric, and ionospheric populations are mixed in the interior boundary layers. This result, which is consistent with previous studies, is now supported by observations of a much broader spectrum of measurements including three-dimensional electron, energetic particle, heavy ion and plasma wave. Some new features are also found: even for quiet subsolar magnetopause crossings, transient or small-scale structures still occur sporadically; slight heating may occur in the boundary layers. Some outstanding issues are clarified by this study: the electron flux enhancements in the lowest energies in the boundary layers and magnetosphere are ionospheric electrons and not photoelectrons from the spacecraft; for northward IMF, they are photoelectrons, but for southward IMF they may be secondary electrons; and the density measurements from differential and integral techniques are similar, leaving no room for a significant "invisible" population.

1. INTRODUCTION

The magnetopause at the subsolar point for strongly northward interplanetary magnetic field (IMF) is an interface between two magnetized plasmas with nearly parallel magnetic fields and without a significant relative motion. Although in MHD theory this interface can be treated mathematically as an infinitely thin separatrix which separates two distinct solutions [e.g., *Crooker*, 1985], the magnetic field and plasma change over a finite interval and not necessarily coincidently. The field transition occurs in current layers and the particle transition can be abrupt over gyroradius or less scales or occur in a broader region called a boundary layer. Previous theoretical investigations [*Ferraro*, 1952; *Parker*, 1967; *Sestero*, 1966; *Alpers*, 1969; *Lee and Kan*, 1979; *Whipple et al.*, 1984] considered the situation when these two transitions are coincident and thin. Observations of the low-latitude boundary layer (LLBL), which is a layer filled with magnetosheath particles but occurring on the magnetospheric side of the magnetopause current layer [*Hones et al.*, 1972; *Eastman et al.*, 1976; al *Haerendel et. al.*, 1978; *Paschmann*, 1979; *Sckopke et al.*, 1981; *Mitchell et al.*, 1987], suggest that the particle transition is not always coincident with the field transition. However, this apparent independence may be due to the paucity of fully integrated studies of the particle and field behvarior. Any study of the magnetopause must study both the field transition and particle transition.

In a series of studies, *Paschmann et al.* [1986, 1990, 1993] and *Sonnerup et al.* [1987] also reported the differences of the magnetopause and boundary layer structures for different IMF orientations. In the course of our observational investigation, we have found that the three-dimensional nature of the interface and dynamic processes, such as reconnection, would affect greatly the structure of the interface. The model described by *Song and Russell* [1992] reflects partly the complexity of this problem. We have started a systematic investigation to further our understanding of the magnetopause. The approach of the investigation is as follows: (1) starting with the subsolar region where the effects of the flow are minimal, (2) examining the extreme IMF conditions, when the fields on the two sides of the interface are either parallel or antiparallel, (3) studying the crossings when the magnetopause was not in rapid motion in order to increase the spatial resolution of the measurements, and (4) using information from a variety of instruments. The initial results of this approach have been reported by *Song et al.* [1990]. They presented the data from three instruments for a slow magnetopause crossing when the IMF was strongly northward. Many questions have been raised concerning the conclusions of that work. The most frequent question is how representative that case is. Other concerns are more technical, such as how to determine the motion of the magnetopause by using a single spacecraft and how to exclude the possible existence of "invisible" populations. In this study we extend our previous study in two directions. One is to show more crossings under similar conditions and the other is to include observations from more instruments. We will test the previous

[1]Institute of Geophysics and Planetary Physics, University of California, Los Angeles.
[2]The High Altitude Observatory, National Center for Atmospheric Research, Boulder, Colorado.
[3]NASA Goddard Space Flight Center, Greenbelt, Maryland.
[4]Los Alamos National Laboratory, Los Alamos, New Mexico.
[5]Applied Physics Laboratory, The Johns Hopkins University, Laurel, Maryland.
[6]Lockheed Palo Alto Research Laboratory, Palo Alto, California.
[7]University of Washington, Seattle.
[8]Department of Physics and Astronomy, University of Iowa, Iowa City.
[9]Departement de Recherche Spatiale, Observatoire de Paris, Meudon, France.

Paper number 93JA00606.
0148-0227/93/93JA-00606$05.00

TABLE 1. Parameters for Three Subsolar Magnetopause Crossings

Year	Day	Time, UT	Location, R_E, GSM	N_{SW}, cm^{-3}	V_{SW}, km/s	ρV_{SW}^2, nPa	IMF, nT, GSM	L_{STL}, km	L_{OBL}, km	L_{IBL}, km	l, km
1978	Nov. 1	1521	(10.9, 0.0, 0.6)	9.6	386	2.41	(0.5, 2.4, 4.5)	500–1300	380–1000	170–430	10–25
1977	Nov. 5	1714	(10.4, -1.1, 5.2)	6.9	330	1.3	(-3.7, 4.4, 3.6)	~2000	~670	~720	$\lesssim$60
1977	Nov. 24	1936	(9.5, -5.9, 5.0)	7.7	288	1.1	(3.7, -1.1, 2.6)			~800	$\lesssim$120

L_{STL}, L_{OBL}, and L_{IBL}; thicknesses of the sheath transition layer, and outer and inner boundary layers, respectively; l; thickness of the sharp boundary between layers.

results on this new basis. Because more instruments bring in more phenomena, another objective of this paper is to understand the relationship among different phenomena and among different instruments. This understanding of the relationship can be used later in some more complicated situations and different areas.

In this study we examine three ISEE magnetopause crossings which occurred near the subsolar region when the IMF was strongly northward. We examine the structure and properties of the magnetopause, using measurements from 10 different instruments. In the appendix we briefly discuss the characteristics of each of the instruments used in this study. Although the wave properties for these three crossings are reported separately [*Song et al.*, 1989, 1993*a*, *b*], we will briefly discuss the relationship between the wave properties and particle properties. In section 2, we begin with an overview of the three crossings. Then in section 3 we discuss the definition of the magnetopause. In sections 4 and 5, we show two-dimensional (2-D) and three-dimensional (3-D)

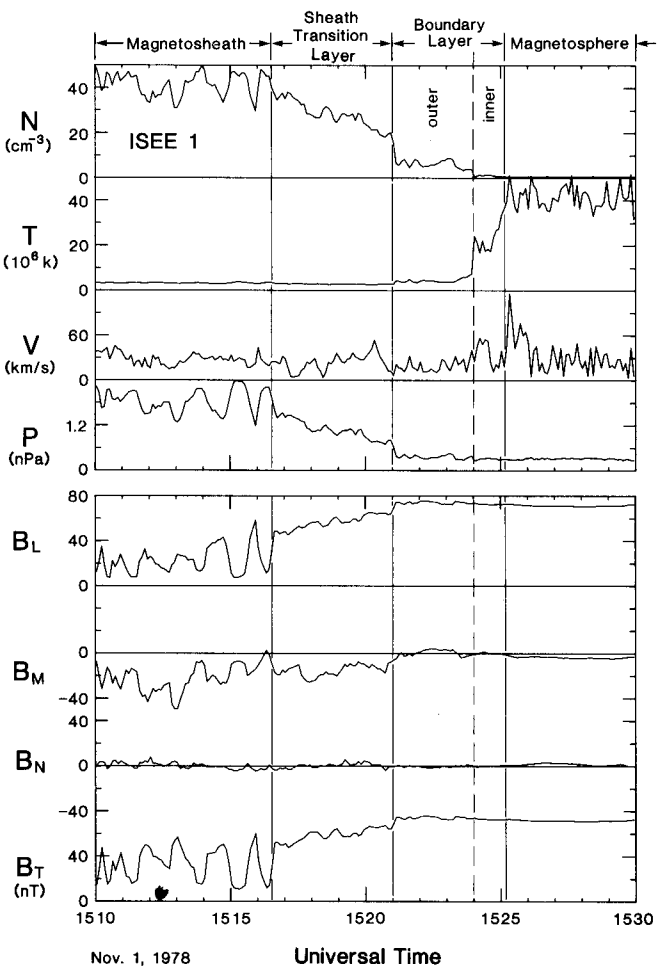

Fig. 1*a*. A slow magnetopause crossing by ISEE 1 on November 1, 1978, after *Song et al.* [1990]. Plasma data with a time resolution of 6 *s* are from the FPE. *N*, *T*, *V*, and *P* are the ion density (cm^{-3}), temperature (10^6 K), ion flow velocity (km/s), and ion pressure (nPa). The magnetic field is presented in the boundary normal coordinates. The tangential discontinuity technique was used to determine the normal direction of the magnetopause. The *N* direction is normal to the boundary and sunward, the *L* direction is tangent to the boundary and along the magnetospheric field, and *M* is along N x L. B_T is the magnitude of the field. Regions are separated by vertical lines. The sheath transition layer is the region the magnetosheath plasma density changes. The outer boundary layer and the inner boundary layer are characterized by the sudden drop in the density and the sudden increase in the temperature.

particle distribution functions. In sections 6 and 7, we show the measurements of the energetic particles and heavy ions. Since the possible existence of an "invisible" population has become one of the major questions concerning magnetopause observations, in section 8, we compare the density measurements from different instruments. The results show that if such an invisible population exists, it is very small.

2. SLOW MAGNETOPAUSE CROSSINGS

The locations of the three magnetopause crossings for northward IMF are shown in Table 1. They are all in the subsolar region.

November 1, 1978, crossing. Figure 1 shows ISEE 1 data from a subsolar magnetopause crossing on November 1, 1978, while ISEE 1 was inbound. We have collected all of the data from ISEE instruments for this crossing. Thus it is the most completely studied crossing. The measurements from the Fast Plasma Experiment (FPE) [*Bame et al.*, 1978], the flux gate magnetometer

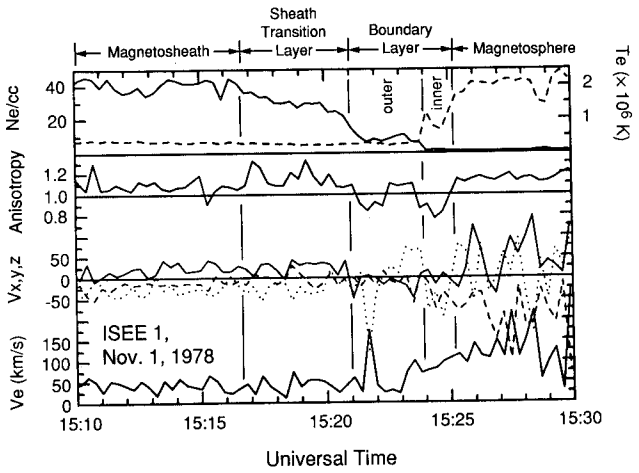

Fig. 1*b*. The three-dimensional electron moments measured by the VES on November 1, 1978. The top panel shows the electron density (solid line), in cm^{-3} and the electron temperature (dashed line), in degrees. The second panel shows the electron temperature anisotropy, the ratio of the perpendicular temperature to the parallel temperature. The third panel shows the three components of the electron velocity, in km/s, in GSE coordinates: V_x (dashed line), V_y (dotted line), and V_z (solid line). The bottom panel shows the magnitude of the electron velocity.

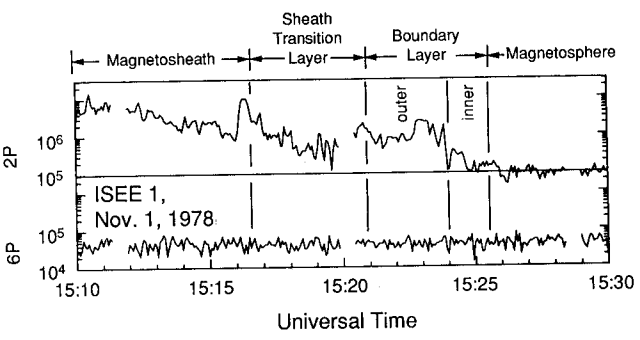

Fig. 1*c*. Proton fluxes, in $cm^{-2}\,s^{-1}\,sr^{-1}$, along the Z direction, GSE, measured by the dual spacecraft energetic particle experiment on November 1, 1978. The center energy is 1.4 keV for channel 2P and 6.0 keV for channel 6P. Channel 2P measures the magnetosheath population and channel 6P is close to the cross point of distributions for different regions, in Figure 4*b* of *Song et al.* [1990]. Flux is similar across the magnetopause for 6P. Electron fluxes are not shown for this crossing because they are in the noise level which is higher than that in 1977.

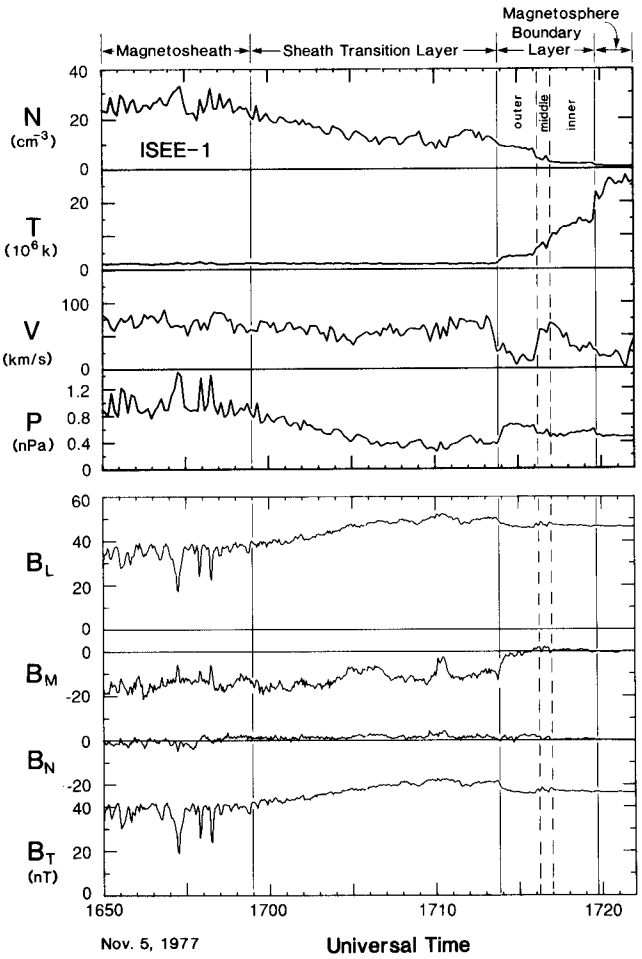

Fig. 2*a*. Measurements for a slow magnetopause crossing by ISEE 1 on November 5, 1977, in the same format as Figure 1*a*.

[*Russell*, 1978], the electric field [*Mozer et al.*, 1978] and IMF and solar wind conditions for this crossing have been reported by *Song et al.* [1990]. Electron data are from the Vector Electron Spectrometer (VES) [*Ogilvie et al.*, 1978]. Three-dimensional ion measurements derived from combining the FPE and Lepedea [*Frank et al.*, 1978] data are shown by *Song et al.* [1993b]. The ion and electron fluxes along the spacecraft spin axis are measured at fixed energies by the Dual Spacecraft Energetic Particle Experiment [*Anderson et al.*, 1978]. The wave properties for this crossing can be found in the work of *Song et al.* [1989, 1990, 1993*a*]. The different appearance between the ion density measured by the FPE and the electron density by the VES is due to the lower time resolution of the VES. The higher electron velocity is caused by the z component of the velocity which was not measured by the FPE. One might speculate that the rapid change at 1521 UT is the magnetopause current layer. Since the current layer is 500~2000 km thick according to the work of *Berchem and Russell* [1982] and this change occurs in about 5 s, the current layer should be in rapid motion. Using the field strength of 74 nT, the inferred electric field associated with this motion should be from 7.4 to 21.6 mV/m tangent to the boundary and perpendicular to the magnetic field. Since the magnitude of the measured DC electric field is less than 2 mV/m [*Song et al.* 1990] throughout the crossing, the change at 1521 UT itself cannot be the magnetopause current layer as defined by *Berchem and Russell* [1982]. The measured flow velocity is also inconsistent with the above speculation because it requires a normal velocity of 100 km/s which is not observed. The measured normal

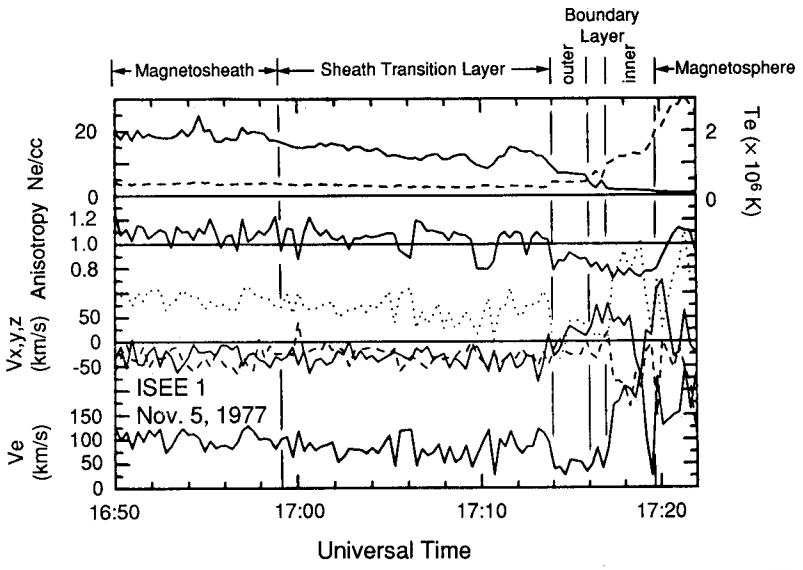

Fig. 2*b*. Electron moments measured by the VES on November 5, 1977 in the same format as Figure 1*b*.

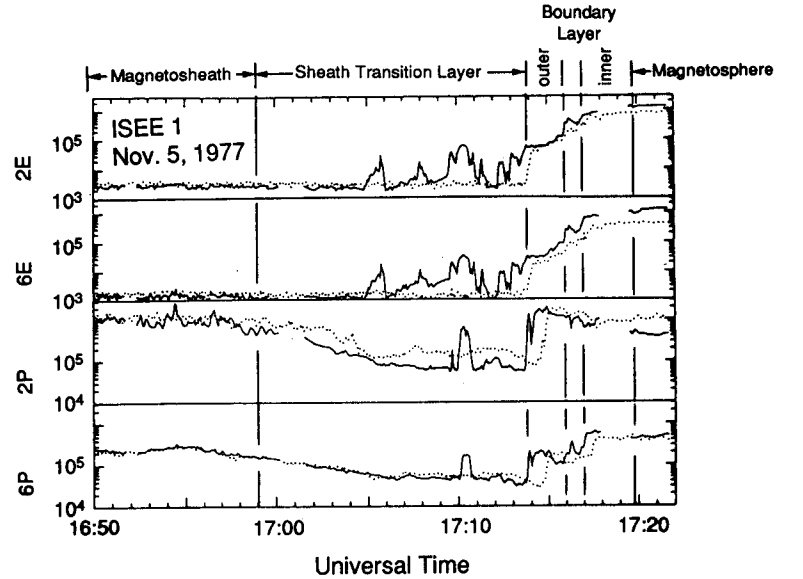

Fig. 2*c*. Flux, in $cm^{-2}\ s^{-1}\ sr^{-1}$, along the Z direction measured from the dual-spacecraft energetic particle experiment on November 5, 1977. Solid lines are for ISEE 1 and dashed lines are for ISEE 2. The fluxes are measured from narrow-band detectors: 2E and 6E are for electrons, and 2P and 6P are for ions. The center energy is 1.4 keV for 2E, 5.6 keV for 6E, 1.4 keV for 2P, and 6 keV for 6P.

component of the flow velocity was less than 5 km/s relative to the spacecraft. In section 6 we estimate the thickness of the sharp boundary between the two boundary layers using the finite Larmor gyroradius effect and show that the boundary moved with a speed of 2 to 4 km/s. The estimated thicknesses for each layer are shown in Table 1.

November 5, 1977, crossing. Figure 2 shows a magnetopause crossing near the subsolar point on November 5, 1977 by ISEE 1. This crossing has been reported by *Russell and Elphic* [1978], *Paschmann et al.* [1978], and *Parks et al.* [1978]. We will study this crossing with measurements from more instruments. Three dimensional ion measurements are shown by *Song et al.* [1993*b*]. The normal direction is (0.835, -0.190, 0.516) GSE. The separation of ISEE 2 from ISEE 1 was (-259, 174, -215) km GSE. The measurements from IMP 8 indicate that the IMF is northward during the interval of the crossing. The temperature and density change in steps from the sheath transition layer to the magnetosphere similar to the crossing on November 1, 1978. The changes in the density and temperature at each sharp boundary measured by ISEE 2 FPE are consistently 72 s later than those measured by ISEE 1 (not shown). Similar features can be found in Figure 2*c* from the Dual Spacecraft Energetic Particle Experiment. This indicates that the thickness of the boundary layers does not change significantly during the interval of the crossing and that there is no dramatic change in the motion of the boundary. Therefore the rapid changes between layers are spatial rather than temporal features. The reduced velocity of the boundary is 5 km/s and sunward. The sharp boundaries between the layers are about 60 km thick. There is a small-scale transient phenomenon near 1710 UT. It was only seen by ISEE 1 and not by ISEE 2.

November 24, 1977, crossing. Figure 3 shows our third crossing for the northward IMF. The normal vector is (0.781, -0.423, 0.459) GSE. Since the separation distance from ISEE 2 to ISEE 1 is (223, -353, 192) km GSE, the separation along the normal is 412 km. The solar wind and IMF were monitored by IMP 8 at (4.4, -36.8, 19.6) R_E GSM shown in Table 1. The IMF was northward with a large radial component. There are no significant

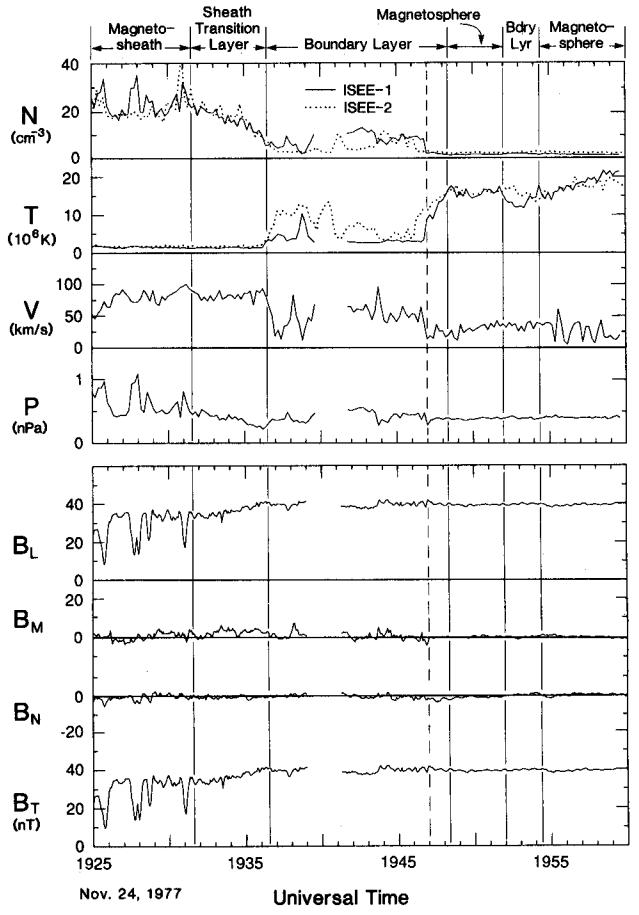

Fig. 3*a*. Measurements for a slow magnetopause crossing by ISEE 1 (solid lines) and ISEE 2 (dashed lines) on November 24, 1977, in the same format as Figure 1*a*.

changes in either the IMF or the solar wind during this magnetopause crossing. There are fluctuations in the ion temperature, most obviously seen in the ISEE 2 data from about 1936 UT to about 1942 UT. The cause of the fluctuations is unknown. The time delay between the encounters of the inner edge of the outer boundary layer for the two spacecraft is about 40 s. Thus the velocity of this sharp boundary is about 10 km/s and its thickness is less than 120 km. It is difficult to estimate the thickness of the boundary layer and the sheath transition layer for this crossing because of the perturbations that occurred in between these boundaries.

3. Definition of the Magnetopause

There are several definitions, or so-called "working definitions," of the magnetopause in previous studies essentially based on the responses of different instruments. The differences among these definitions become important for studies of the magnetopause structure. In usual magnetopause crossings, since the sheath transition layer and its edges cannot be resolved because of the fast motion of the magnetopause, which results in a low spatial resolution of the measurements, the rapid change in the field associated with both the sheath transition layer and its edges can be identified as a single magnetopause current layer. However, when the magnetopause is moving slowly and the edges of the sheath transition layer can be resolved, using the same definition that the magnetopause current layer is the last rapid change in the field, which is the outer edge of the sheath transition layer for the crossings of November 1, 1978, and November 24, 1977, and is the inner edge of the sheath transition layer for the crossing of November 5, 1977, the sheath transition layer becomes a sublayer of the magnetospheric boundary layer for the crossings of November 1, 1978, and November 24, 1977, though there is no change in the plasma population. The difficulties in defining the magnetopause are also recognized in a recent study of the structure of low shear magnetopause [*Paschmann et al.*, 1993]. They found from AMPTE/IRM data that the "key time" when plasma temperature and distribution function undergo a rapid change is associated with almost no change in the field for magnetopause crossings with small magnetic shear, which is the same as our strongly northward IMF cases. Their "key time" is the same as our inner edge of the sheath transition layer. It becomes obvious that to define the magnetopause as the current layer proposed in early highly simplified theoretical models is not appropriate because there is no current present for a boundary

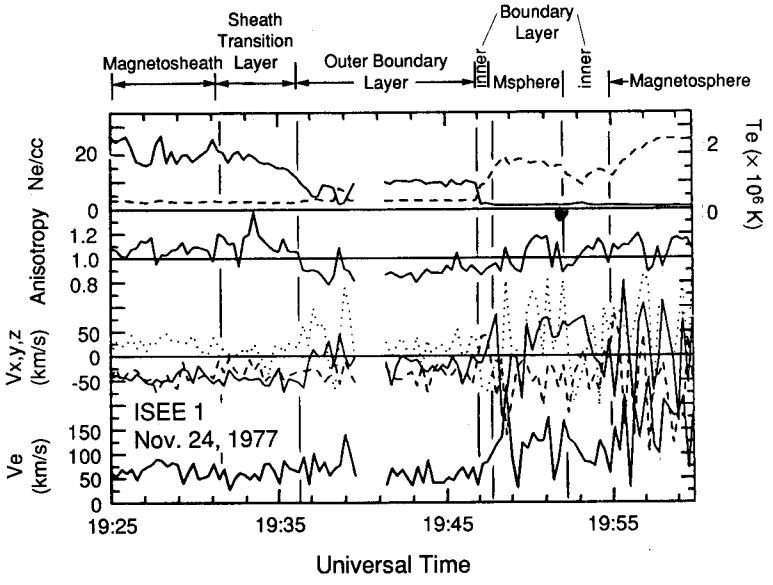

Fig. 3*b*. Electron moments measured by the VES on November 24, 1977, in the same format as Figure 1*b*.

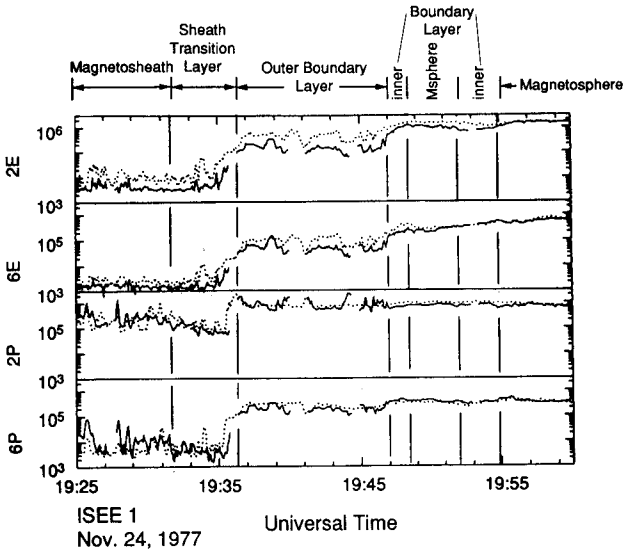

Fig. 3c. Flux along the Z direction measured from the dual-spacecraft energetic particle experiment on November 24, 1977, in the same format as Figure 2c.

separating two distinct magnetized plasmas with equal thermal pressures. Even worse, as pointed out by Paschmann et al. and in the discussion above, electric current may flow outside the "magnetopause" if we define the "key time" as the magnetopause. If we have to redefine the magnetopause, we suggest that the new definition should (1) have clear physical meaning, (2) be applicable to a variety of situations, e.g., with or without reconnection, and (3) if possible, be applicable to different measurements. Although the inner edge of the sheath transition layer, or the "key time" of Paschmann et al., has clear physical meaning, i.e., separating the region in which magnetosheath population is dominant from that with significant presence of magnetospheric and ionospheric populations, it does not describe the entire function of the magnetopause as discussed by Paschmann et al., is ambiguous when reconnection occurs, and is not applicable to some instruments, such as plasma wave measurements and energetic particle measurements. Our suggestion to solve this problem is to define the magnetopause as a region. In our study, we define the magnetopause as the transition region from the magnetosheath field and particles to the magnetospheric field and particles. This definition is physical, i.e., including the entire physical function of the magnetopause, and is applicable to any circumstance. This whole transition will leave its footprint on every relevant instrument. The differences within each part of the magnetopause are not important for many studies. For studies in which these differences become essential, a reference time, or "key time," is necessary to align different events. Multiple instruments are required for these studies at least before the establishment of the relationship among different signatures from different instruments. One may wish to call the sheath transition layer the depletion layer since it is associated with a decrease in the density. However, this is only true for a strongly northward IMF. For a strongly southward IMF, the same region, i.e., the field transition region, may not be associated with a depletion [*Paschmann et al.*, 1979, *Song et al.*, 1989]. The density and temperature measurements from the FPE and magnetic field measurements show the same profile for our three crossings. The lines separating the different regions in Figures 1, 2, and 3 are drawn based on the magnetic field and FPE measurements. Measurements from most instruments usually show consistent changes but some of them may be relatively gradual.

In general the magnetopause contains two regions: the field transition region, or the sheath transition layer, and the particle transition region. The particle transition is broader. In the magnetosheath side of the sheath transition layer, there are still magnetospheric energetic particles. The sheath transition layer itself also hosts part of the particle transition, observable mainly in the density. A more dramatic particle transition is seen in the magnetospheric side of the sheath transition layer and has been referred to as the LLBL in most previous studies; it is referred to as simply the boundary layer in this study. The sharp changes in the plasma properties separate each sublayer. These rapid changes, compared with the relatively smooth layers, in the bulk of the plasmas are best seen in the FPE and are referred to as sharp boundaries or edges of a layer in our discussion. The outer edge of the sheath transition layer may not be well defined sometimes. In general, based on the FPE and magnetic field measurements, the outer edge is associated with a change in the type of the waves, or a decline in Pc 3-4 waves and an enhancement in Pc 1 waves from the magnetosheath to the sheath transition layer for northward IMF. As will be discussed later in this paper, the distribution function of the particles and properties of the VLF waves also change from layer to layer. In this paper and companion studies [*Song et al.*, 1989, 1993*a, b*] we study the relationship between the various types of wave activity and particle distribution functions. Then the high time resolution wave measurements can be used as diagnostics of the particle distribution.

In our definition, for northward IMF, the sheath transition layer and its edges are the same as the magnetopause current layer of *Russell and Elphic* [1978] and *Berchem and Russell* [1982] and the depletion layer of *Paschmann et al.* [1978, 1993]. The sharp boundary between the sheath transition layer and the outer boundary layer is the "magnetopause" of *Paschmann et al.* [1978], the "key time" of *Paschmann et al.* [1993] and most of other studies of the LLBL using particle data. The outer and inner boundary layers are similar to the LLBL and halo [*Sckopke et al.*, 1981], respectively.

4. TWO-DIMENSIONAL DISTRIBUTIONS

Figure 4 shows the 2-D contour plots of the ion distribution functions for the crossing on November 5, 1977, from ISEE 2. The contour plots for the crossing on November 1, 1978, are not available and those for November 24, 1977, crossing are similar to Figure 4, not shown. The measurements are from the FPE, and one distribution, measured in 3 s, is selected for each region within and near the magnetopause. The FPE measures the flux ±55° from the ecliptic plane. Although the FPE is not sensitive to the temperature anisotropy when the field is almost along the spin axis, it provides some information about the anisotropy since the magnetospheric dipole field still has a small component projected on this plane. The angle between the field and the normal of the ecliptic plane is 26.9° for the crossing. In the magnetosheath, the particles are cool with a convective motion and the anisotropy is not significant. In the sheath transition layer, it is the same population as seen in the magnetosheath but with a smaller density and larger anisotropy. The 3-D ion measurements shown by *Song et al.* [1993*b*] for the three crossings indicate that the temperature anisotropy is about 1.2 to 1.5 in the magnetosheath and about 2 or greater in the sheath transition layer. *Anderson et al.* [1991] showed similar features in an

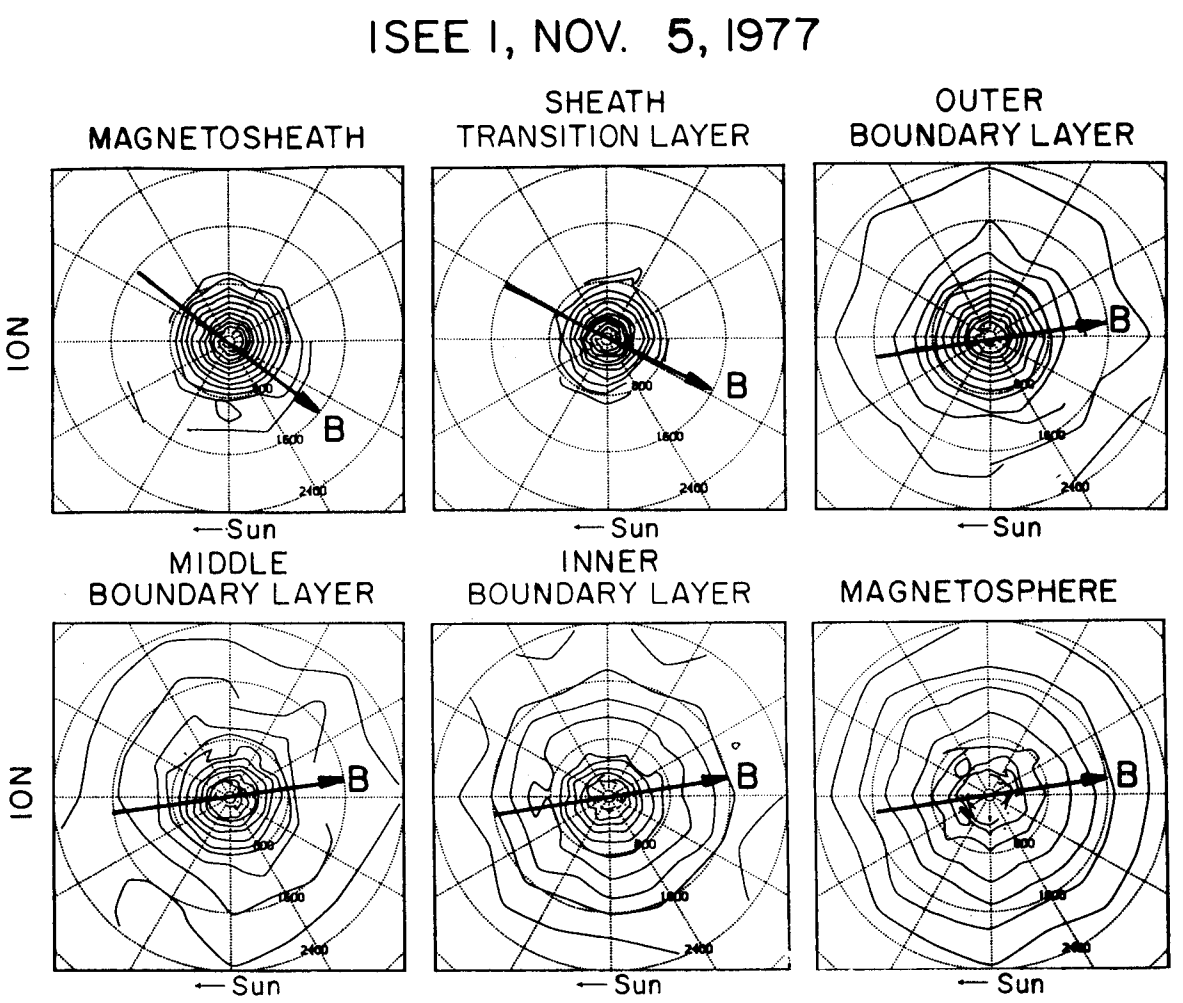

Fig. 4. Distribution contours for ions measured by the FPE on ISEE 1 on November 5, 1977. The distribution is measured in the GSE x-y plane. The dotted circles indicate equal velocity as labeled value, km/s, in phase space. Direction of the magnetic field projected on the x-y plane is shown for reference.

AMPTE/CCE magnetopause crossing when the IMF is strongly northward. In the outer boundary layer, the hot population starts to appear while the cool population decreases. In the inner boundary layer the hot population becomes dominant. In the magnetosphere, the cool population disappears completely.

Figures 5*a* and 6*a* compare the ion distribution functions for each region in and near the magnetopause for the two crossings in 1977. The same plot for the November 1, 1978, crossing can be found in Figure 4 of *Song et al.* [1990]. These distributions are measured from the FPE and averaged over azimuth to have better statistics. A heating process in a certain layer is important if the distribution for this layer is above both of those for the magnetosheath and magnetosphere; i.e., the population in this layer cannot be supplied by the magnetosheath and magnetosphere, and must be provided through heating [*Song et al.*, 1990; *Traver et al.*, 1991] An example of a significant heating process can be found when the IMF is strongly southward [*Song et al.*, 1989]. For the November 5, 1977, and November 24, 1977, crossings, the distribution for the outer boundary layer is slightly higher than others near 1 keV. This is also shown in Figures 2*c* and 3*c* in channel 2P and may be caused by a heating process although it is not significant in the overall change in the plasma. Figures 5*b* and 6*b* compare the electron distribution functions for the two crossings in 1977. Slight heating in $\gtrsim$ 100-eV electrons is seen in the boundary layers for the two crossings.

The major difference between the ion distributions and electron distributions is an increase in the lowest energies in the magnetosphere and inner boundary layer for electron distributions. Since these electrons have very low energy, they may be affected by the change in the spacecraft potential. For the crossing on November 1, 1978, the spacecraft is negatively charged with a potential of -4V in the sheath transition layer (C. A. Cattell, private communication, 1990). Since the absolute value of the spacecraft potential is proportional to the temperature of ambient electrons when the spacecraft is not positively charged [e.g., *Chen*, 1974, p. 295], the increase in the ambient electron temperature from the outer boundary layer to the magnetosphere is associated with a spacecraft potential drop. This potential drop deepens the potential well for electron access to the spacecraft. The electrons have higher energy than measured energy. Thus the real distribution for the boundary layers and magnetosphere should be shifted to higher energies, not to lower energies. In other words, the features observed in the lowest energies should not be a hidden feature revealed by changing the spacecraft potential. The observed low-energy population is certainly not the low-energy portion of the magnetosheath particles since it has a different

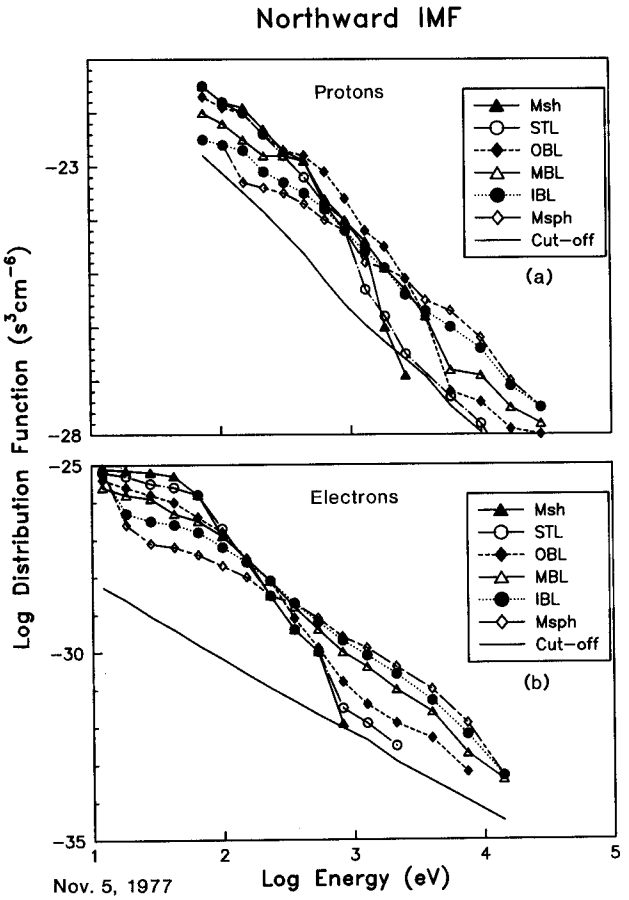

Fig. 5. (*a*). Ion distribution function showing slices through the distribution functions for the regions in and near the magnetopause from the FPE on November 5, 1977, from ISEE 1. The distribution functions are averaged in the equatorial plane. (*b*) Electron distribution functions.

shape of the distribution in the corresponding energies. Therefore it must be due to photoelectrons or secondary electrons. The photoelectrons have very low energies, less than 20 eV, since there are few photons available from the sun with an energy larger than 27 eV (460 angstroms) [e.g., *Gibson*, 1973]. Here we recall that the ionization energy for a hydrogen atom from the fundamental state is 13.6 eV and the work function for most of metals is around 6 eV. The observed low-energy electrons are not due to the photoelectrons from the spacecraft since they have much greater flux than can be provided by the spacecraft. Thus these electrons can only come from the ionosphere by traveling along the field lines.

There are two ionospheric electron populations, photoelectrons and secondary electrons. The secondary electrons are produced by the ionospheric ionization due to the bombardment of the precipitating ions. The spectra are different for the two populations. The slope is about 3 for the secondary electrons and 4~5.2 for the photoelectrons [*Fung and Hoffman*, 1991]. The slopes for our cases are about 6.5. Thus these electrons are most likely to be the ionospheric photoelectrons. *Song et al.* [1989] showed a similar spectral analysis for a southward IMF crossing. The slope for that crossing is 3.2 and hence most likely caused by secondary electrons. Therefore it is possible that ionospheric electrons seen at low latitudes are primarily photoelectrons for northward IMF and secondary electrons for southward IMF. The presence of the ionospheric electrons is an indication that the inner boundary layer field connects to the ionosphere. We will show further evidence that the inner boundary layer is located on closed field lines and the outer boundary layer may be located on newly closed field lines from 3-D electron, the energetic particle, and the heavy ion measurements in the next three sections, since this is one of the most important issues in our study.

5. Three-Dimensional Electron Distributions

Three-dimensional electron distributions can be measured by the VES and the medium energy particles experiment (MEPI). Since these two instruments measure different energy ranges, we will discuss them separately. First we discuss the VES measurements. From the 2-D electron distributions, Figures 4*b* of *Song et al.* [1990], and Figures 5*b* and 6*b*, we have shown that the electron distributions across the magnetopause cross each other at 100 ~ 300 eV. This energy can be used to distinguish between the particles of magnetosheath origin and those of magnetospheric origin. Since the VES measures electrons from a few eV to 2 keV, it provides a good coverage of the magnetosheath population and a partial coverage of the magnetospheric population, and it is more sensitive to the ionospheric photoelectrons. Figure 7 shows the time series of the electron distribution function contours for the crossing of November 1, 1978. The distribution has been averaged over directions. The contours near 100 ~ 300 eV are nearly straight from the magnetosheath to the magnetosphere and hence separate the magnetosheath population from the magnetospheric one. Above these lines, the contours go up and below these lines they go down from the magnetosheath to the magnetosphere. Being consistent with the measurements from the FPE, the distribution changes sharply at edges between layers and remains

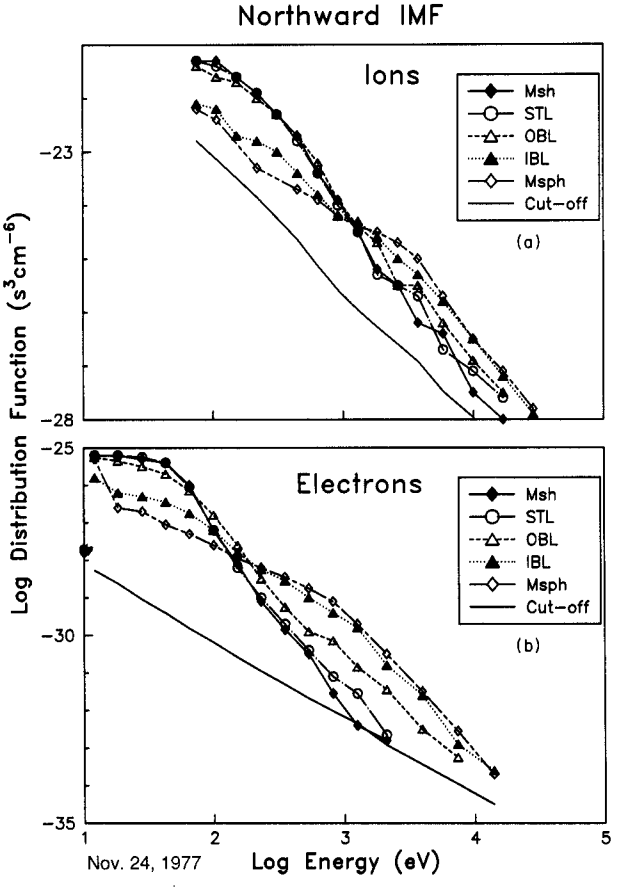

Fig. 6. Distribution slices on November 24, 1977, ISEE 1, in the same format as Figure 5.

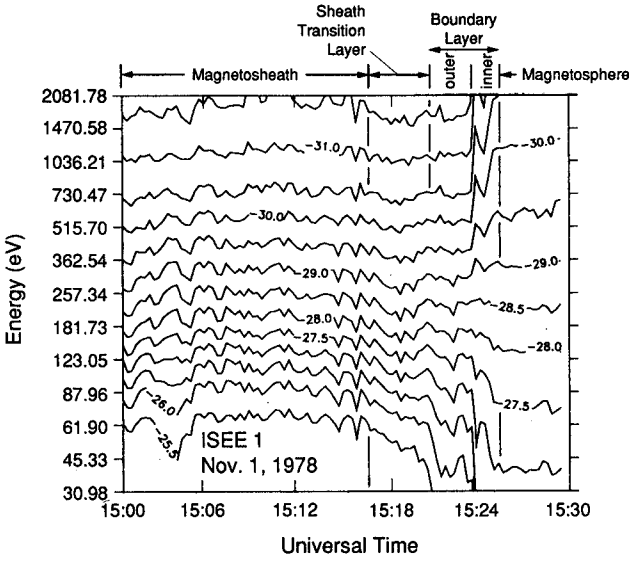

Fig. 7. Time series of electron distribution contours measured from the VES for the crossing of November 1, 1978. The distribution is averaged in 3-D. The energy for which the distribution has similar values on both sides of the magnetopause separates the population of magnetosheath origin and that of magnetospheric origin.

relatively constant within each layer. The high-energy flux does not increase until the sharp boundary between the two boundary layers for the crossing of November 1, 1978. For the crossing of November 5, 1977 (not shown), there is a sharp increase in the medium energies at the boundary between the sheath transition layer and the outer boundary layer. The flux increase for higher energies is at the boundary between the two boundary layers. For the crossing of November 24, 1977 (not shown), the flux increase for medium and high energies is at both the boundary between the sheath transition layer and the outer boundary layer and the boundary between the two boundary layers. *Fuselier et al.* [1989] and *Anderson et al.* [1991] reported cases similar to the November 24, 1977, crossing. A heating process in a layer can be identified when a contour is higher in the layer than in both the magnetosheath and magnetosphere. Consistent with the discussion in the last section, there is no notable heating for the November 1, 1978, crossing, and slight heating is observed in the boundary layers near 200 eV for the two 1977 crossings.

Figures 8, 9, and 10 show the 3-D distributions for the three crossings and one distribution is shown for each region. The magnitude of the electron distribution function is slightly different between that from the FPE and that from the VES because of the difference in calibration and aging for the two instruments. In the magnetosheath and sheath transition layer, the anisotropies for lower energies and for higher energies are similar. However, they become more and more different from the outer boundary layer to the inner boundary layer and to the magnetosphere. The fluxes with lowest energies become more parallel to the field and the fluxes with highest energies become perpendicular to the field. In the inner boundary layer and magnetosphere, even beams parallel and antiparallel to the field are clearly seen in the energy around 10 eV. The energy of this population was best measured in November 24, 1977, crossing during which the instrument was operated in a mode to measure lower energies. This is the feature expected due to the ionospheric photoelectrons and is a characteristic for field lines which connect with the ionosphere. Since there are many photoelectrons at energies around 10 eV available in the ionosphere, these photoelectrons can move along the field lines from the ionosphere to the spacecraft and become more field-aligned as the field strength decreases from the ionosphere to low latitudes. They cause the large flux along the field. Because these photoelectrons are seen in both parallel and antiparallel directions, the field lines must connect with both northern and southern hemisphere, closed field lines. Above, we have shown that these lowest-energy electrons are ionospheric photoelectrons and that the inner boundary layer is located on closed field lines. Since the fluxes at these lowest energies in the outer boundary layer are still higher than the fluxes in the inner boundary layer associated with the ionospheric photoelectrons, we have not shown conclusively whether the outer boundary layer is located on closed or open field lines. However, there is an increase in the parallel fluxes at the lowest energies from the sheath transition layer; the outer boundary layer may be on newly closed field lines where filling of the ionospheric electron is undertaken or on the field lines which have only one end connecting with the ionosphere. On the other hand, for closed magnetospheric field lines, high-energy particles continuously fill the loss cone and are lost into the ionosphere due to the pitch angle diffusion [*Kennel and Petscheck*, 1966] associated with the VLF waves observed in these regions [*Song et al.*, 1989]. Thus more high-energy particles should appear perpendicular to the field lines. We can see this feature partly in Figures 8, 9, and 10 and will see this more dramatically in the MEPI measurements in the next section.

An interesting feature of these three-dimensional distribution contours is that there is a plateau, where the distribution contour becomes vertical over a large perpendicular velocity range, at about 700 eV, or in the vicinity of the parallel velocity equal to 15×10^3 km/s, for distributions in the boundary layers and magnetosphere. It is the evidence of pitch angle diffusion processes associated with VLF waves seen in these regions. There are electrostatic waves of a frequency near $3/2\, f_{ce}$ in these regions. These waves are the Bernstein mode [e.g., *Kennel and Ashour-Abdalla,* 1982]. They propagate nearly perpendicular to the field and have the perturbed electric field along the wavevector. This perturbed electric field is fed by the particle energy. Thus the resonant particles lose their perpendicular energy without changing their parallel energy. This causes the plateau in the distribution contours. Since current theory does not provide the determination of the resonant energy, or the parallel component of the wavevector, we cannot verify our observations with theory. From this observation, the resonant energy appears to be 700 eV. The pitch angle diffusion associated with these waves should provide the ionospheric precipitating electrons and cause part of the dayside soft auroral missions.

Figure 11 shows the ratio, α, of the flux perpendicular to the field to the flux parallel to the field as functions of energy and time for the crossing of November 1, 1978. The solid lines are for α=0.5 and the dotted lines α=2.0. Thus the regions of solid lines, shaded, are with a larger parallel flux, the regions of dotted lines a larger perpendicular flux, and the empty regions nearly isotropic. In the magnetosheath and the sheath transition layer, it is isotropic in the lowest energies. There is a perpendicular anisotropy in the medium energies. In the outer boundary layer, a parallel anisotropy is seen in the medium energies. In the inner boundary layer and magnetosphere, there is a parallel anisotropy in the lower energies and there is a perpendicular anisotropy in the higher energies. Figure 11 clearly shows the changes in the population which cause the change in the temperature anisotropy at the key time of *Paschmann et al.* [1993].

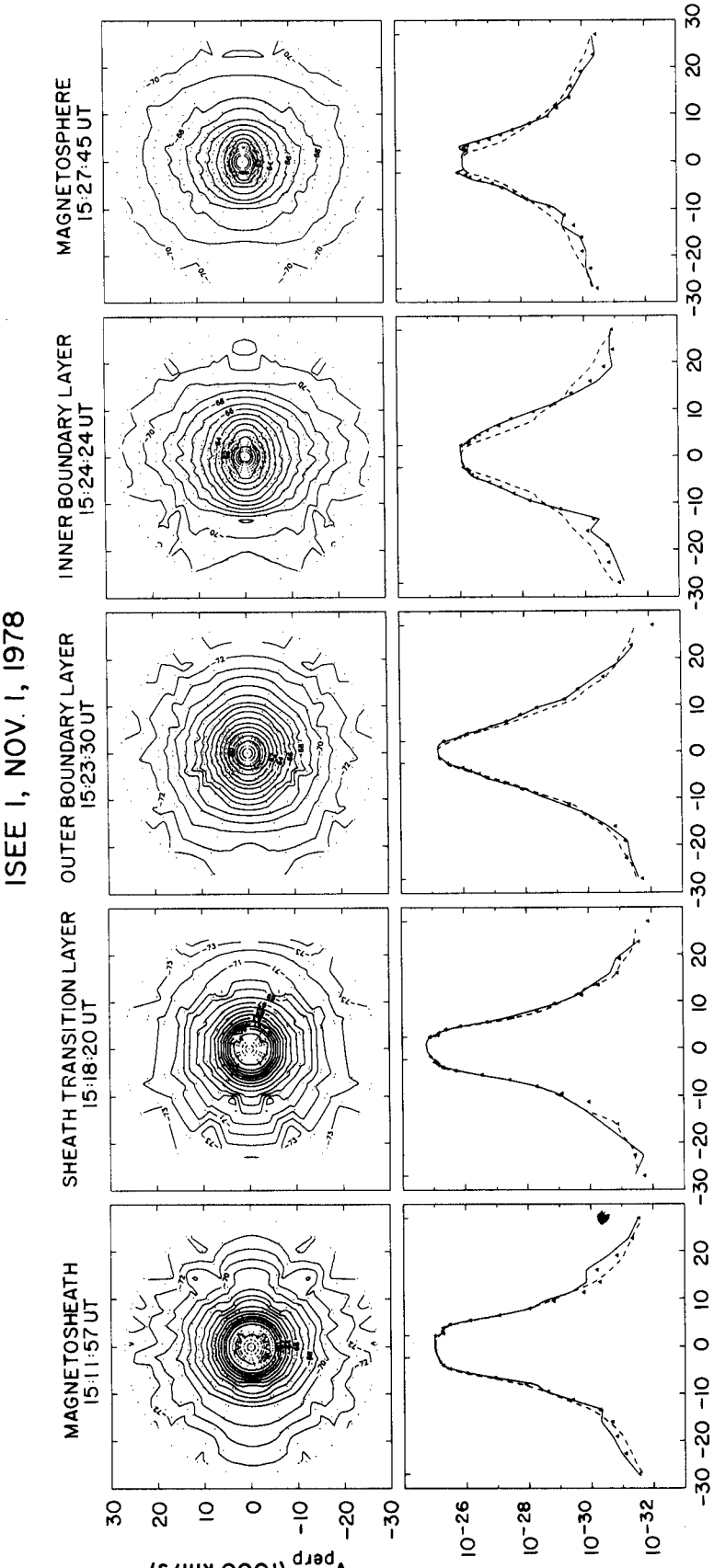

Fig. 8. The upper panel shows electron distribution contours parallel and perpendicular to the magnetic field derived from 3-D electron measurements by the VES on November 1, 1978. The values of the contour are natural logarithm of the distribution function, (in s^3 cm^{-6}). The lower panel shows the cuts of the distribution. Solid lines are for parallel and antiparallel, dashed lines are for perpendicular, and the triangles are the actual measurements closest to the parallel and antiparallel directions.

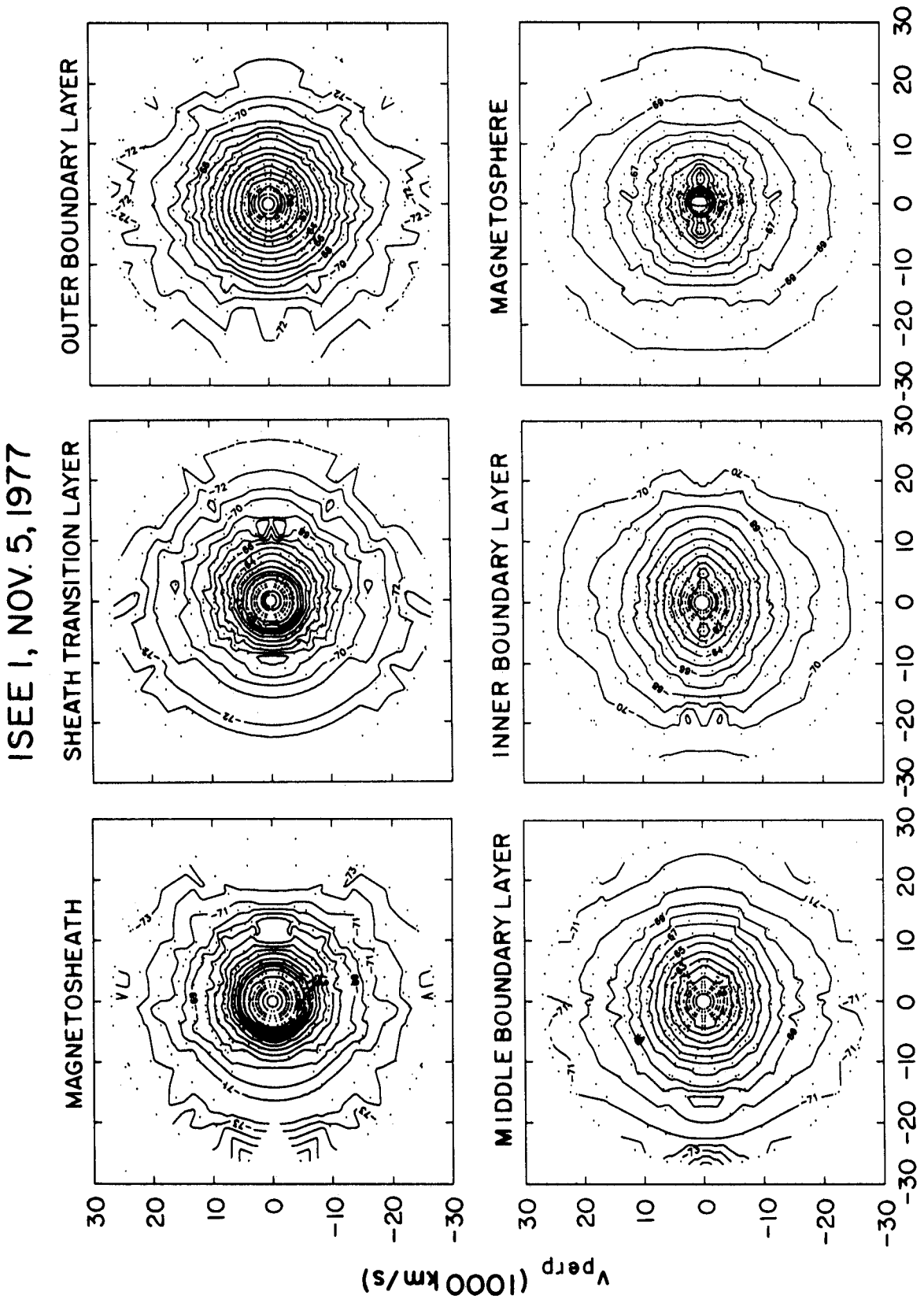

Fig. 9. Electron distribution contours parallel and perpendicular to the field on November 5, 1977.

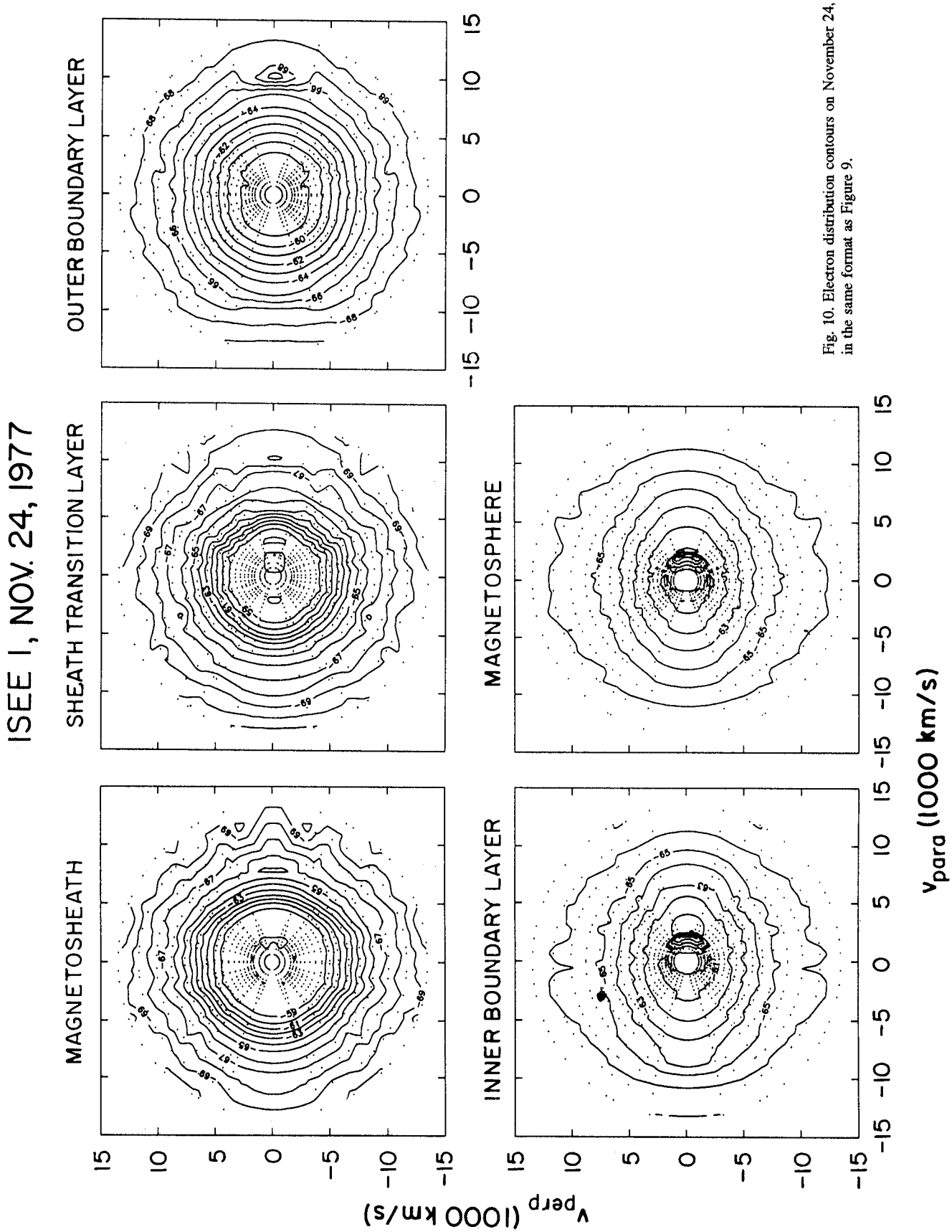

Fig. 10. Electron distribution contours on November 24, 1977, in the same format as Figure 9.

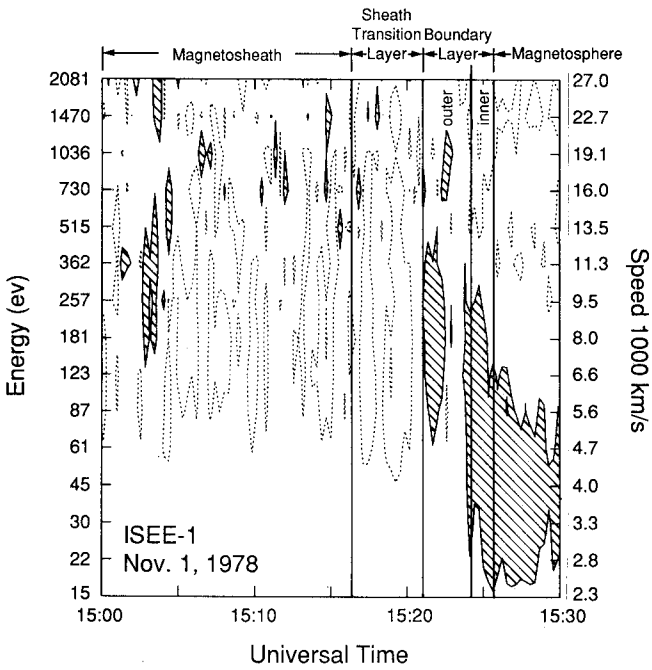

Fig. 11. Contours of the ratio, α, of the perpendicular flux to the parallel flux, solid lines α=0.5 and dotted lines α=2.0. The shaded regions indicate an anisotropy along the field.

6. ENERGETIC PARTICLES

Figure 12 shows energetic electron and proton fluxes measured by the MEPI and averaged for each complete scan, 36 s, for the crossing of November 1, 1978. These energetic particles are of magnetospheric origin and the fluxes decrease from the magnetosphere to the magnetosheath. The gyroradii of the particles from the top trace are 5.7 km, 7.7 km, 10.2 km, 260 km, 600 km, and 720 km. The corresponding energies are 31, 57, 98, 34, 55, and 80 keV. The flux changes more sharply for particles with smaller gyroradii and the particles with larger gyroradii can

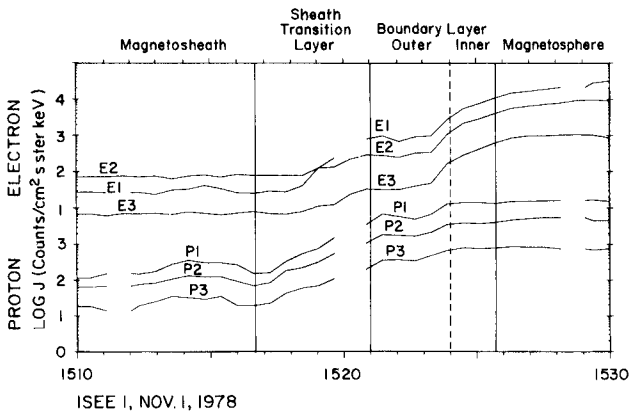

Fig. 12. Fluxes measured from the MEPI on November 1, 1978. The top three traces are from three electron energy channels, 22.5 ~ 39 keV for E1, 39 ~ 75 keV for E2, and 75 ~ 120 keV for E3, respectively. On the magnetosheath side, the fluxes are in the noise level. E2 has a higher noise level than E1. The bottom three traces are from three ion energy channels, 24 ~ 44.5 keV for P1, 44.5 ~ 65.3 keV for P2, and 65.3 ~ 95.5 keV for P3, respectively. The fluxes are averaged for each complete scan, 32 s.

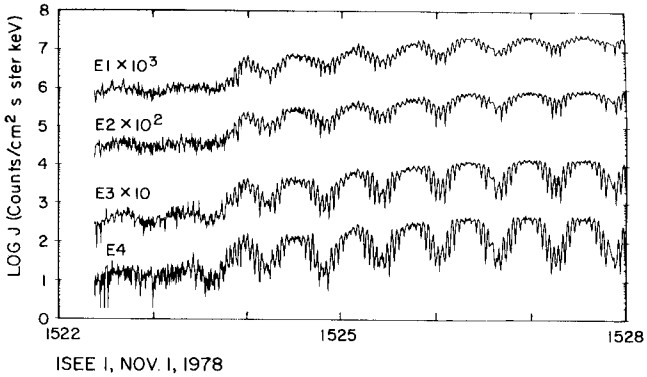

Fig. 13. Fluxes for four electron channels of the MEPI with full time resolution, 3/8 s per sample, across the sharp boundary between the outer and inner boundary layers. The high-frequency modulation after 1524 UT is caused by the spin of the spacecraft, and the low-frequency modulation by the scan in elevation. Higher fluxes indicate the detector is more perpendicular to the background magnetic field.

penetrate farther from the magnetosphere. The electron fluxes are close to the noise level in the magnetosheath. Some of the energetic ions are present in the magnetosheath side of the sheath transition layer. We will not discuss this region, since it has little effect on the overall transition processes for northward IMF, but it shows that the particle transition is more complicated and extends to a much larger region than the field transition [*Williams*, 1979; *Sibeck et al.*, 1987]. Figure 13 shows full time resolution electron fluxes. The fluxes in the inner boundary layer and magnetosphere are strongly modulated by the spacecraft spin period, 3 s, and scan period, 36 s. It reaches the maxima when measured perpendicular to the magnetic field. Thus these energetic particles are trapped particles on closed field lines. This anisotropy in high-energy particles is very important for the whistler waves observed by *Song et al.* [1989]. There is a sudden flux change at the edge between the outer and inner boundary layers. The anisotropy decreases from the inner boundary layer to the outer boundary layer are more prominent for lower energies than for higher energies. This feature provides us a unique opportunity to determine the thickness of the sharp boundary between the two boundary layers.

Let us assume that there is a scattering mechanism confined to a region with a thickness *D*. A particle with a gyroradius smaller than *D*/2 will be scattered completely and its pitch angle will become random after it crosses the region. Thus a trapped distribution will become isotropic after the scattering. However, if the gyroradius of the particle is larger than D/2, it may not be scattered completely and can keep some of its original anisotropy after the scattering. Since the gyroradius is 5.7 km for channel E1 and 10.2 km for channel E3, we estimate the thickness between the two boundary layers to be 10 ~ 20 km, which is about two to four hybrid gyroradii of the background plasma and is much smaller than the ion gyroradius of the background plasma. We have used this result to determine the velocity of the magnetopause relative to the spacecraft in section 2 and it is consistent with other measurements and previous statistical studies.

7. HEAVY IONS

Heavy ions can be used as diagnostics of the origin of the plasma. The ions in which we are interested are H^+, He^{++}, He^+, and O^+. Since the solar wind is a highly ionized plasma, it

TABLE 2. Ion Composition at the Magnetopause on November 24, 1977

	He^{++}, cm^{-3}	He^{++}/H^+, %	He^+, cm^{-3}	He^+/H^+, %	O^+, cm^{-3}	O^+/H^+, %
Msheath	0.52	1.4	0.004	0.01	0	0
Sheath TL	0.43	1.7	0.004	0.02	0	0
Outer BL	0.06	0.6	0.053	0.38	0.015	.10
Inner BL			0.009	0.39	0.015	.67
Msphere	0.01	0.8	0.018	1.1	0.047	1.8

contains little He^+ and O^+. Most of the He^+ and O^+ ions are of ionospheric origin [*Peterson et al.*, 1982] and the ratio of He^{++}/H^+ is lower for the population of ionospheric origin than that of solar wind origin. Therefore a significant flux of O^+ and He^+ and a smaller ratio of He^{++}/H^+ indicates that the plasma is on field lines connected to the ionosphere. The plasma composition experiment [*Shelley et al.*, 1978] was operated in a variety of modes. Only on November 24, 1977, was it operated in a mode which is appropriate to our study in our three crossings. Table 2 shows the composition measurements in different regions of the magnetopause for this crossing. The normalization of the heavy ion densities is obtained by dividing the heavy ion densities by the proton density measured from the FPE during the intervals when the heavy ion density is measured. The flux of He^{++} is high in the magnetosheath and sheath transition layer and is low in the boundary layers and magnetosphere. The He^+ and O^+ fluxes are just the opposite. This result is consistent with the measurements from other instruments and within the range of the results shown recently by *Eastman et al.* [1990] from AMPTE/CCE magnetopause crossings. Thus the particles in the sheath transition layer are almost purely from the magnetosheath and the boundary layers are combinations of the magnetosheath, ionospheric, and magnetospheric plasmas.

8. COMPARISON OF THE DENSITY MEASUREMENTS

Since no particle instrument can cover the whole energy range and all three dimensions, there are uncertainties in the determination of the density from particle measurements. One can always surmise the existence of an invisible population for a particular instrument. This possible "invisible" population has become one of the major uncertainties in understanding the magnetopause. In this section we compare the densities measured from different instruments.

Ideally, the electron density can be accurately measured from the plasma frequency. In reality, due to a finite frequency bandwidth of the wave detector, there is uncertainty in the density measurement. However, this density measurement has not been widely used in magnetopause studies. The Electron Density Experiment (EDE) [*Harvey et al.*, 1978] measures accurately the average electron density between ISEE 1 and 2. When the separation between the two spacecraft is not too large, the average density can be used as the local density. However, this instrument was not operated continuously. The Vector Electron Spectrometer provides a direct electron density measurement. This measurement is three-dimensional and includes electrons down to 10 eV. The Fast Plasma Experiment provides two-dimensional electron and ion density measurements. *Song et al.* [1993*a*] have developed a technique to calibrate the FPE ion density against the magnetic field measurements assuming a total pressure balance near the subsolar magnetopause. The comparison among the densities measured from different instruments for the crossing of November 1, 1978, has been shown by *Song et al.* [1993*a*]. For this crossing, since the two spacecraft were separated by a long distance, 7854 km, the electron density experiment did not provide a density measurement. Figure 14 shows the comparison for the two crossings in 1977. Since the frequency resolution for the narrow-band sweep frequency receiver (see appendix) of the Iowa plasma wave experiment is about 7%, the uncertainty in the density measurement is about ±14%, which is about 4 times the size of the circles in Figure 14. Thus the densities measured by the electron density experiment, the plasma wave instrument, the VES, and calibrated FPE are in agreement with each other, with a high precision in 1977. In the November 1, 1978, crossing, the VES density agrees with the plasma wave measurements and the calibrated FPE density is almost identical with the VES density in

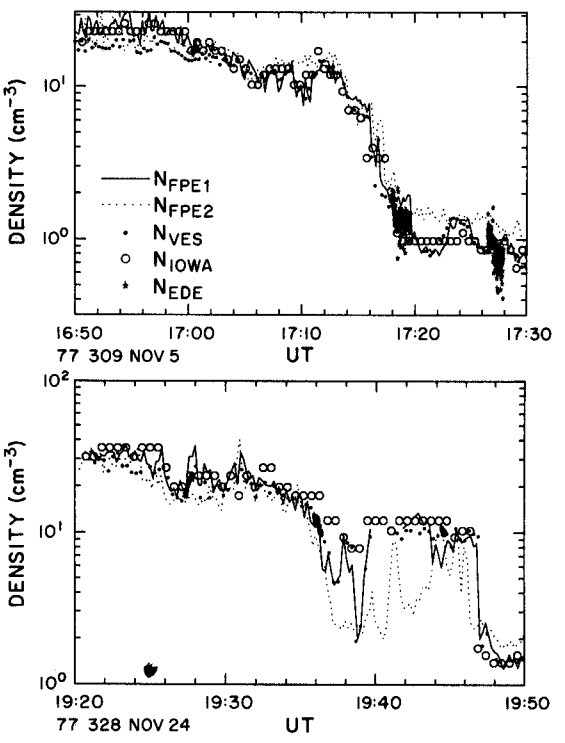

Fig. 14. Comparison of the density measurements from different instruments. The solid line and dotted line are the ion density measured by the FPE and calibrated according to the total pressure balance near the magnetopause from ISEE 1 and 2, respectively. Solid dots are electron density measured by the VES. Open circles are the electron density derived from the plasma wave measurements. The uncertainty is about 4 times the diameter of the circles. Stars, which are clustered near 1700, 1718 and 1727 UT for November 5, 1977, crossing and near 1928, 1936 and 1946 UT for November 24, 1977 crossing, are the average electron density between ISEE 1 and 2 measured from the Electron Density Experiment.

the magnetosheath and the sheath transition layer, although it is lower than the VES density in the magnetosphere where the condition for the calibration does not apply.

The conclusions we can draw from this comparison are as follows: (1) The instruments on ISEE are capable of measuring the plasma near the magnetopause. The invisible population, if any, appears to be unimportant at least for northward IMF cases (2) Total pressure balance is a quantitatively good assumption near the subsolar magnetopause at least for northward IMF.

9. DISCUSSION

Our three subsolar slow magnetopause crossings for strongly northward IMF show that the region containing most of the magnetopause current, the sheath transition layer, is almost completely within the magnetosheath plasma rather than a mixture of the magnetosheath and magnetosphere plasmas. The particles change only in density. This indicates that the field transition is not coincident with the major part of the particle transition near the subsolar region for strongly northward IMF. Since the flow velocity normal to the magnetopause is small, the total pressure, the sum of the particle thermal pressure and magnetic pressure, remains nearly constant across the magnetopause. The density decreases while the field strength increases from the magnetosheath to the boundary layer. Although the plasma depletion may be similar to the effect studied by *Lees* [1964] and *Zwan and Wolf* [1976], as discussed by *Song et al.* [1992] and *Southwood and Kivelson* [1992], the slow mode process in the plasma depletion model should not act through the whole magnetosheath as described by Zwan and Wolf. Associated with the field increase and density decrease, as predicted by *Crooker and Siscoe* [1977], we note that there is an increase in the ion temperature anisotropy in the sheath transition layer [*Anderson et al.*, 1991; *Song et al.*, 1993*b*; *Paschmann et al.*, 1993], which is not included in the depletion model. As reported by *Song et al.* [1990, 1993*b*] and *Anderson et al.* [1991], there are wave enhancements near the ion gyrofrequency in this region, indicating that the kinetic effects may become important in the depletion process. On the other hand, although the sheath transition layer is many ion gyroradii thick, the sharp boundary between the transition layer and outer boundary layer is about a few hybrid gyroradii to an ion gyroradius thick. It separates the region dominated by magnetosheath population from that with significant presence of magnetospheric and ionospheric populations, and hence is specially important.

The particle transition on the magnetospheric side for our three strongly northward IMF crossings is accomplished with more than one boundary layer. Similar observations have also been reported by *Ogilvie et al.* [1984], *Ogilvie and Fitzenreiter* [1989], *Paschmann et al.* [1990], *Takahashi et al.* [1991], *Hall et al.* [1991], and *Paschmann et al.* [1993]. Besides the changes in the density and temperature, there is also a change in the temperature anisotropy at the inner edge of the sheath transition layer. The ion anisotropy is highly perpendicular in the sheath transition layer, but drops in the boundary layers. A weak electron anisotropy in the sheath transition layer becomes parallel to the field in the boundary layers. These features are consistent with the Epoch analysis of *Paschmann et al.* [1993]. The boundary layers are relatively uniform within each one and separated by sharp boundaries. This steplike profile indicates that the transition is not accomplished in one time scale, for example, a diffusion process. Rather, it more likely results from a time dependent process. The inner boundary layer is apparently located on closed field lines. The outer boundary layer contains a significant level of magnetospheric energetic particles and ionospheric heavy ions, while magnetosheath population is still dominant in the density. Because this mixture cannot be produced by diffusion, as discussed just before and as shown in particle simulations [*Winske et al.*, 1991], the boundary layers may be formed through reconnection. In this case, the outer boundary layer may be located on newly closed field lines. VLF wave measurements [*Song et al.*, 1989] may lend further support to this possibility. The electrostatic $3/2\, f_{ce}$ wave, which represents a mixture of a hot population with a cold population and hence may represent field lines connecting to the ionosphere, occurs in the two boundary layers and magnetosphere. The whistler mode chorus, which represents a well-developed loss cone distribution, occurs in the inner boundary layers and magnetosphere but not in the outer boundary layer. Therefore the outer boundary layer may be located on closed field lines but the loss cone distribution has not been well developed, i.e., newly closed field lines. *Song and Russell* [1992] have developed a model to describe a possible process in forming this observed profile. Localized intermittent reconnection may take place at high latitudes. Through the reconnection, the magnetosphere captures flux tubes from the solar wind. The reconnection at the two ends of a flux tube is not necessarily simultaneous. A reconnected flux tube sinks into the magnetosphere associated with propagating Alfven waves and is dispersed into a layer by the interchange motion. Different reconnection events form different sublayers of the boundary layer. These layers represent different ages after reconnection. If there are surface waves on the sharp boundaries between layers and between the boundary layer and magnetosphere, the boundary layer may be observed similarly to what was reported by *Sckopke et al.* [1981]. Reconnection may heat the plasma at the reconnection site. However, since the reconnection site is only a small portion of a flux tube and at high latitudes, the effects of the heating should not be significant seen at low latitudes.

In this paper, we have shown two more examples and added much more experimental details to the description of each crossing in response to the questions raised concerning the conclusion of *Song et al.* [1990]. Although there are minor differences from case to case, the overall structure, the particle properties and wave properties are similar. This similarity is not trivial. The three cases in a similar study we are doing for strongly southward IMF appear very different in plasma properties. This explains why a variety of the phenomena have been reported. Furthermore, the observations from different instruments are consistent with each other, or they can be understood physically. Thus, the cases shown in this study should be representative for subsolar region when the IMF is strongly northward. These cases are in general consistent with other crossings reported under similar conditions. Most features discussed in this paper can be found in the cases presented by *Paschmann et al.* [1993]. For the crossings which are not very close to the subsolar region, the effects due to flow may result in additional features, such as multiple crossings of the sharp boundary between layers. In these cases, the boundary layers may look like several pulses. Since the depletion effect becomes weaker away from the subsolar region, the sheath transition layer may become faint. Because of the growth of some instabilities which may occur in this region, the sharp boundaries between layers may become thicker farther from the subsolar region. For example, the sharp boundary for the November 24, 1977, crossing, which occurred farthest from the subsolar point in our three crossings, is thickest in the three crossings.

10. CONCLUSIONS

We have studied three subsolar magnetopause crossings with data from 10 different instruments when the IMF was strongly northward. The magnetopause for these three crossings shows similar structure. It consists of a sheath transition layer and steplike boundary layers. Heating is insignificant across the magnetopause. These layers are separated by sharp boundaries. This basic structure is supported from a variety of measurements. We have studied the relationship among different phenomena observed by these instruments and tried to understand the processes at the magnetopause coherently. Some of our findings are consistent with our earlier results, but with more extensive support. These include the observation that, in addition to the overall structure, the boundary layers contain a combination of the magnetosheath, magnetospheric, and ionospheric populations, but the sheath transition layer contains basically magnetosheath particles. There are some interesting new features. Even for quiet subsolar magnetopause crossings, transient or small-scale structures still occur sporadically. Slight heating may occur in the boundary layers. The heating does not necessarily take place near the spacecraft when it is passing these regions, since locally we find no evidence for the mechanism which may cause heating, such as cyclotron waves.

With this study, we have gained a much better understanding of the ionospheric electrons. These electrons appear as the flux enhancements in the lowest energies in the boundary layer and magnetosphere and are along the field. For a northward IMF, these electrons are dominated by those of photoionization origin. When the IMF is southward, the secondary electrons caused by the bombardment of the precipitating ions may become most important. Therefore this finding eliminates the association of the electron flux in the lowest energies with the photoelectrons from the spacecraft itself. Another subject we have examined closely is the existence of so-called "invisible" populations. The density measurements from different instruments, some of them independent of either energy range or the field angle of view, are very close to each other, leaving no room for a significant invisible population. We have also discussed a method using the finite Larmor radius effect of energetic particles to determine the thickness of the sharp boundary, which appears to be thinner than an ion gyroradius.

The discussion of the relationship among different phenomena and the physical linkage among different instruments in this study shows a great potential of multiple-instrument studies. Today's observations can provide almost complete information. Coherent physical undestanding of the information can lead to conclusive interpretations and eliminate much speculation.

APPENDIX: INSTRUMENTATION

There are 10 different instruments involved in this paper and its companion studies [*Song et al.*, 1989, 1990, 1993*a*, *b*]. These instruments cover most of the frequency and energy ranges of interest. Table 3 summarizes the major features of these instruments.

The magnetometer [*Russell*, 1978] measures the vector magnetic field from both ISEE 1 and 2. In the magnetosheath and outer

TABLE 3. Instruments for the Magnetopause Study

Name	Quantity	S/C[a]	Dimension	Range	Field Angle[b], deg	Rate[c]	Reference [1978]
Flux gate	B	1/2	3-D	0~2 Hz		1/4	*Russell*
SDP	E	1	2-D	0~4 Hz		1/8	*Mozer et al.*
				(6 Hz, 32Hz, 256 Hz)			
FPE	ion	1/2	2-D	75 eV to 20 keV	110	12	*Bame et al.*
	electron			12 eV to 20 keV			
MEPI	ion	1	3-D	>24 KeV	14	36	*Williams et al.*
	electron			>20 KeV			
VES	electron	1	3-D	11~2062 eV	5	16	*Ogilvie et al.*
IOWA	δE	1/2		5.62 Hz to 311 kHz		1	*Gurnett et al.*
	δB			5.62 Hz to 10 kHz			
LEPEDEA	ion	1	3-D	234 eV to 41 keV	38[d]	16/scan	*Frank et al.*
	electron			239 eV to 42 keV			
PCE	heavy ion	1	2-D	1~150 amu	10	3	*Shelley et al.*
DEPE	ion	1/2	1-D	1.4, 5.7 keV		1/4	*Anderson et al.*
	electron			1.4, 6.0 keV			
EDE	Ne	1/2					*Harvey et al.*

[a]S/C; spacecraft.
[b]Only in latitude.
[c]Low data rate, in seconds.
[d]Near the equator.

magnetosphere, the accuracy of the measurements is 1/128 nT. These measurements are used to determine the background magnetic field and low-frequency magnetic fluctuations for both ISEE 1 and 2.

The spherical double probes [*Mozer et al.*, 1978] measure the electric field on the plane perpendicular to the spacecraft spin axis from ISEE 1. This instrument also provides the spacecraft potential and three channels of wave measurements. Since the spacecraft potential is negatively proportional to the electron temperature when the spacecraft is negatively charged and is proportional to the electron flux when the spacecraft is positively charged, it can be used as a monitor of the electron measurements. The measurements from the spherical double probes are used to determine the background electric field and the low-frequency electric field fluctuations. The background electric field can be used to monitor the plasma velocity measurements according to the frozen-in condition. At low frequencies the ideal MHD assumption is usually valid, and we can determine the three components of the electric field combining the electric and magnetic field measurements by using $\mathbf{E} \cdot \mathbf{B} = 0$. The measurements of the electric field associated with this study are shown by *Song et al.* [1990, 1993*a*].

The Iowa plasma wave experiment [*Gurnett et al.*, 1978] provides high-frequency electric and magnetic field measurements from both ISEE 1 and 2. There is a high time resolution spectrum analyzer covering a frequency range from 5.62 Hz to 311 kHz with 20 channels. The magnetic field measurements are from a triaxial search coil antenna from 5.62 Hz to 10 kHz with 14 channels. These plasma wave measurements are shown by *Song et al.* [1989]. There is also a narrow-band sweep frequency receiver covering the frequency range from 100 Hz to 400 kHz. The time resolution for this measurement is low, 32 s, but the frequency resolution is high, 6.5%. We use this measurement to determine the electron density.

From the above three instruments, we can obtain full spectra of waves for both electric and magnetic fields. Particle measurements are more complicated. There are many instruments. Each of them is designed for a special purpose.

The fast plasma experiment (FPE) [*Bame et al.*, 1978] measures low-energy electrons and protons with high time resolution in the plane perpendicular to the spacecraft spin axis from both ISEE 1 and 2. Sixteen energy channels are equally distributed in the logarithmic energy scale. Since its energy range covers the bulk of the magnetosheath populations, the FPE provides good measurements of plasma moments in the magnetosheath with relatively high time resolution. In the magnetosphere, since the hot population becomes important, the first moment, the velocity, and the second moment, the temperature, are not measured accurately. Two-dimensional distribution measurements for both electrons and ions are very useful in qualitative studies.

The energetic particles are measured by the medium energy particles experiment (MEPI) [*Williams et al.* 1978] from ISEE 1. The MEPI provides three-dimensional energetic electron and ion measurements. Since most energetic particles are inside the magnetosphere, the MEPI is very useful to monitor the magnetosphere population. Since the MEPI is a 3-D instrument, it provides pitch angle distribution, which is important to study VLF waves and to determine open or closed field lines. Because the Larmor radius is large for energetic particles, these particles can be used as remote sensing for the properties of large scales.

The Vector Electron Spectrometer (VES) [*Ogilvie et al.*, 1978] employs six electrostatic detectors, each with 8.5° x 11° fields of view, looking in each sense along three mutually orthogonal directions fixed in the ISEE 1 spacecraft. The electron energy range at each detector is divided into 16 steps. Since its energy range is lower than that of the FPE electron measurements, the VES provides good measurements for the magnetosheath population. The time resolution of the VES is moderately high. The electron moments, anisotropy, and pitch angle distribution measurements are very important for studying the plasma waves.

The low-energy proton and electron differential energy analyzers (LEPEDEA) [*Frank et al.*, 1978] provide low time resolution 3-D electron and proton measurements. The LEPEDEA works in a different manner than other particle instruments. It has seven detectors looking at different elevations and samples the azimuthal angle while the spacecraft spins. It samples one energy level in a complete scan, in 4 s, then changes to the next energy level. To make a complete measurement, over 32 energy levels, it takes 128 s in the high data rate and 8.5 min in the low data rate. Although the low time resolution and high-energy range are not ideal for studies of the magnetopause structure, *Song et al.* [1993*b*] have developed a method combining the LEPEDEA measurements with the FPE measurements to calculate three-dimensional quantities when the IMF is in strongly north-south directions.

The heavy ions can be measured by the Plasma Composition Experiment [*Shelley et al.*, 1978] from ISEE 1. It is a 2-D instrument measuring the particle fluxes in the plane perpendicular to the spin axis. This instrument has a variety of operating modes. Only a few of them are useful for our study. We use this instrument to identify the region where the field lines connect the ionosphere, or the region on closed field lines.

The Dual Spacecraft Energetic Particle Experiment [*Anderson et al.*, 1978] consists of two identical instruments on the ISEE 1 and 2. These two instruments have very small field angle, high time resolution, and two fixed energy channels for electrons and for protons. This experiment measures only the flux antiparallel to the spacecraft spin axis. Thus the measurements from the two spacecraft can provide good relative timing for the encounters of a boundary by the two spacecraft.

The plasma density can also be measured by the EDE [*Harvey et al.*, 1978]. This experiment measures the phase velocity of a radio wave of frequency 683 kHz transmitted from ISEE 1 and received by ISEE 2. The phase velocity is measured by comparing the phase of the wave received at the ISEE 2 with the phase of the same wave modulated onto a carrier of frequency high enough to be unaffected by the intervening plasma. This phase difference is proportional to the integral electron density between the two spacecraft. In principle, this experiment provides most accurate density measurements with high time resolution. However, since there is an ambiguity of 2π in the phase determination, for large separation this ambiguity is not easy to resolve. Another disadvantage of this experiment is that it operates only less than 10% of the time. There are many gaps in the data. It is used only as calibration in our study. In the later years of the ISEE mission, EDE was operated continuously one out of 16 orbits. In this latter operation mode, the experiment can be used for many different studies. Since it interfered with the Iowa plasma wave instrument and MEPI, we cannot use this mode in our multiple-instrument study.

Acknowledgments. The authors thank the principal investigators, K. W. Ogilvie, J. D. Scudder, S. J. Bame, G. Paschmann, D. J. Williams, E. G. Shelley, K. A. Anderson, D. A. Gurnett, and C. C. Harvey, for allowing us to examine their data. The analysis of the ISEE magnetic field data at UCLA was originally supported by the National Aeronautics and Space

Administration. Presently the analysis is being supported by the National Science Foundation under grant ATM91-11913 as part of the GEM initiative. The research at Lockheed was funded through NASA under contract NAS5-31217. The work at LANL was performed under the auspices of the United States Department of Energy and supported by NASA under S-04039-D. The work at APL was supported by the NASA contract to the APL/JHU and the Department of the Navy under task I2UOS10 contract NOOO24-85-C-5384. The effort at the University of Iowa was supported by grant NAG5-1093 from the NASA Goddard Space Flight Center. We thank NSSDC for the use of the solar wind and IMF data. P. S. wishes to thank Art Richmond for his careful reading of the draft of this paper and many useful comments, and Liz Boyd for her assistance in preparing the draft.

The Editor thanks two referees for their assistance in evaluating this paper.

REFERENCES

Alpers, W., Steady state charge neutral models of the magnetopause, *Astrophys. Space Sci.*, *5*, 425, 1969.

Anderson, B. J., S. A. Fuselier, and D. Murr, Electromagnetic ion cyclotron waves observed in the plasma depletion layer, *Geophys. Res. Lett.*, *18*, 1955, 1991.

Anderson, K. A., R. P. Lin, R. J. Paoli, G. K. Parks, C. S. Lin, H. Reme, J. M. Bosqued, F. Martel, F. Cotin, and A. Cros, An experiment to study energetic particle fluxes in and beyond the Earth's outer magnetosphere, *IEEE Trans. Geosci. Electron.*, *GE-16*, 213, 1978.

Bame, S. J., J. R. Asbridge, H. E. Felthauser, J. P. Glore, G. Paschmann, P. Hemmerich, K. Lehmann, and H. Rosenbauer, ISEE 1 and 2 fast plasma experiment and the ISEE 1 solar wind experiment, *IEEE Trans. Geosci. Electron.*, *GE-16*, 216, 1978.

Berchem, J., and C. T. Russell, The thickness of the magnetopause current layer: ISEE 1 and 2 observations, *J. Geophys. Res.*, *87*, 2108, 1982.

Chen, F. F., *Introduction to Plasma Physics and Controlled Fusion*, vol. 1, 420 pp., Plenum Press, New York, 1974.

Crooker, N. U., A split separator line merging model of the dayside magnetopause, *J. Geophys. Res.*, *90*, 12,104, 1985.

Crooker, N. U., and G. L. Siscoe, A mechanism for pressure anisotropy and mirror instability in the dayside magnetosheath, *J. Geophys. Res.*, *82*, 185, 1977.

Eastman, T. E., E. W. Hones, Jr., S. J. Bame, and J. R. Asbridge, The magnetospheric boundary layer: Site of plasma, momentum and energy transfer from the magnetosheath into the magnetosphere, *Geophys. Res. Lett.*, *3*, 685, 1976.

Eastman, T. E., E. A. Greene, S. P. Christon, G. Gloeckler, D. C. Hamilton, F. M. Ipavich, G. Kremser, and B. Wilken, Ion composition in and near the frontside boundary layer, *Geophys. Res. Lett.*, *17*, 2031, 1990.

Ferraro, V. C. A., On the theory of the first phase of a geomagnetic storm: A new illustrative calculation based on a idealized (plane, not cylindrical) model field distribution, *J. Geophys. Res.*, *57*, 15, 1952.

Frank, L. A., D. M. Yeager, H. D. Dwens, K. L. Ackerson, and M. R. English, Quadrispherical LEPEDEAS for ISEE's-1 and -2 plasma measurements, *IEEE Trans. Geosci. Electron.*, *GE-16*, 221, 1978.

Fung, S. F., and R. A. Hoffman, A search for parallel electric fields by observing secondary electrons and photoelectrons in the low-altitude auroral zone, *J. Geophys. Res.*, *96*, 3533, 1991.

Fuselier, S. A., W. K. Peterson, D. M. Klumpar, and E. G. Shelley, Entry and acceleration of He^+ in the low latitude boundary layer, *Geophys. Res. Lett.*, *16*, 751, 1989.

Gibson, E. G., The Quiet Sun, *NASA Spec. Publ.*, *SP-303*, p. 281, 1973.

Gurnett, D. A., F. L. Scarf, R. W. Fredricks, and E. J. Smith, The ISEE 1 and ISEE 2 plasma wave investigation, *IEEE Trans. Geosci. Electron.*, *GE-16*, 225, 1978.

Haerendel, G., G. Paschmann, N. Sckopke, H. Rosenbauer, and P. C. Hedgecock, The frontside boundary layer of the magnetosphere and the problem of reconnection, *J. Geophys. Res.*, *83*, 3195, 1978.

Hall, D. S., C. P. Chaloner, D. A. Bryant, V. P. Tritakis, and D. R. Lepine, Electrons in the boundary layers near the dayside magnetopause, *J. Geophys. Res.*, *96*, 7869, 1991.

Harvey, C. C., J. Etcheto, Y. De Javel, R. Manning and M. Petit, The ISEE electron density experiment, *IEEE Trans. Geosci. Electron.*, *GE-16*, 231, 1978.

Hones, E. W., Jr., J. R. Asbridge, S. J. Bame, M. D. Montgomery, S. Singer, and S. I. Akasofu, Measurements of magnetotail plasma flow made with Vela 4B, *J. Geophys. Res.*, *77*, 5503, 1972.

Kennel, C. F., and M. Ashour-Abdalla, Electrostatic waves and the strong diffusion of magnetospheric electrons, in *Magnetosphere Plasma Physics*, edited by A. Nishida, p. 245, D. Reidel, Hingham Mass., 1982.

Kennel, C. F., and H. E. Petschek, Limit on stably trapped particle fluxes, *J. Geophys. Res.*, *71*, 1-28, 1966.

Lee, L. C., and J. R. Kan, A unified kinetic model of the tangential magnetopause structure, *J. Geophys. Res.*, *84*, 6417, 1979.

Lees, L., Interaction between the solar plasma wind and the geomagnetic cavity, *AIAA J.*, *2*, 1576, 1964.

Mitchell, D. G., F. Kutchko, D. J. Williams, T. E. Eastman, L. A. Frank, and C. T. Russell, An extended study of the low-latitude boundary layer on the dawn and dusk flanks of the magnetosphere, *J. Geophys. Res.*, *92*, 7394, 1987.

Mozer, F. S., R. B. Torbert, U. V. Fahleson, C.-G. Falthammar, A. Gonfalone, and A. Pedersen, Measurements of quasistatic and low frequency electric fields with spherical double probes on the ISEE-1 spacecraft, *ISEE Trans Geosci. Electron.*, *GE-16*, 258, 1978.

Ogilvie, K. W., and R. J. Fitzenreiter, The Kelvin-Helmholtz instability at the magnetopause and inner boundary layer surface, *J. Geophys. Res.*, *94*, 15,113, 1989.

Ogilvie, K. W., J. D. Scudder, and H. Doong, The electron spectrometer on ISEE 1, *IEEE Trans. Geosci. Electron.*, *GE-16*, 261, 1978.

Ogilvie, K. W., R. J. Fitzenreiter, and J. D. Scudder, Observations of electron beams in the low-latitude boundary layer, *J. Geophys. Res.*, *89*, 10,723, 1984.

Parker, E. N., Confinement of a magnetic field by a beam of ions, *J. Geophys. Res.*, *72*, 2315, 1967.

Parks, G. K., C. Gurgiolo, C. S. Lin, K. A. Anderson, R. P. Lin, F. Martel, and H. Reme, Dual spacecraft observations of energetic particles in the vicinity of the magnetopause, bow shock, and interplanetary medium, *Space Sci. Rev.*, *22*, 765, 1978.

Paschmann, G., Plasma structure of the magnetopause and boundary layer, in *Magnetospheric Boundary Layers, Eur. Space Agency Spec. Publ. ESA SP-148*, 25, 1979.

Paschmann, G., N. Sckopke, G. Haerendel, I. Papamastorakis, S. J. Bame, J. R. Asbridge, J. T. Gosling, E. W. Hones, Jr., and E. R. Tech, ISEE plasma observations near the subsolar magnetopause, *Space Sci. Rev.*, *22*, 717, 1978.

Paschmann, G., B. U. O. Sonnerup, I. Papamastorakis, N. Sckopke, G. Haerendel, S. J. Bame, J. R. Asbridge, J. T. Gosling, C. T. Russell, and R. C. Elphic, Plasma acceleration at the Earth's magnetopause: Evidence for reconnection, *Nature*, *282*, 243, 1979.

Paschmann, G., I. Papamastorakis, W. Baumjohann, H. Sckopke, C. W. Carlson, B. U. Ö. Sonnerup, and J. Luhr, The magnetopause for large magnetic shear: AMPTE/IRM observations, *J. Geophys. Res.*, *91*, 11,049, 1986.

Paschmann. G., B. Sonnerup, I. Papamastorakis, W. Baumjohann, N. Sckopke, and H. Luhr, The magnetopause and boundary layer for small magnetic shear: Convection electric fields and reconnection, *Geophys. Res. Lett.*, *17*, 1829, 1990.

Paschmann, G., W. Baumjohann, N. Sckopke, T.-D. Phan, and H. Luhr, Structure of the dayside magnetopause for low magnetic shear, *J. Geophys. Res.*, in press, 1993.

Peterson, W. K., E. G. Shelley, G. Haerendel, and G. Paschmann, Energetic ion composition in the subsolar magnetopause and boundary layer, *J. Geophys. Res.*, *87*, 2139, 1982.

Russell, C. T., The ISEE 1 and 2 fluxgate magnetometers, *ISEE Trans. Geosci. Electron.*, *GE-16*, 239, 1978.

Russell, C. T., and R. C. Elphic, Initial ISEE magnetometer results: Magnetopause observations, *Space Sci. Rev.*, *22*, 681, 1978.

Sckopke, N., G. Paschmann, G. Haerendel, B. U. O. Sonnerup, S. J. Bame, T. G. Forbes, E. W. Hones, Jr., and C. T. Russell, Structure of the low-latitude boundary layer, *J. Geophys. Res.*, *86*, 2099, 1981.

Sestero, A., Vlasov equation study of plasma motion across magnetic fields, *Phys. Fluids*, *9*, 2006, 1966.

Shelley, E. G., R. D. Sharp, R. G. Johnson, J. Geiss, P. Eberhardt, H. Balsiger, G. Haerendel, and H. Rosenbauer, Plasma composition experiment on ISEE-A, *IEEE Trans. Geosci. Electron., GE-16*, 266, 1978.

Sibeck, D. G., R. W. McEntire, A. T. Y. Lui, R. E. Lopez, S. M. Krimigis, R. B. Decker, L. J. Zanetti, and T. A. Potemra, Energetic magnetospheric ions at the dayside magnetopause: Leakage or merging?, *J. Geophys. Res.*, *92*, 12,097, 1987.

Song, P., and C. T. Russell, A model of the formation of the low-latitude boundary layer, *J. Geophys. Res.*, *97*, 1411, 1992.

Song, P., C. T. Russell, N. Lin, R. J. Strangeway, J. T. Gosling, M. Thomsen, T. A. Fritz, D. G. Mitchell, and R. R. Anderson, Wave and particle properties of the subsolar magnetopause, in *Physics of Space Plasmas (1989), SPI Conf. Proc. and Reprint Ser.*, edited by T. Chang, G. Crew, and J. Jasperse, p. 463, Scientific Publishers, Inc., Cambridge, Mass., 1989.

Song, P., R. C. Elphic, C. T. Russell, J. T. Gosling, and C. A. Cattell, Structure and properties of the subsolar magnetopause for northward IMF: ISEE observations, *J. Geophys. Res.*, *95*, 6375, 1990.

Song, P., C. T. Russell, and M. F. Thomsen, Slow mode transition in the frontside magnetosheath, *J. Geophys. Res.*, *97*, 8295, 1992.

Song, P., C. T. Russell, R. J. Strangeway, J. R. Wygant, C. A. Cattell, D. J. Fitzenreiter, and R. R. Anderson, Wave properties near the subsolar magnetopause: Pc 3-4 energy coupling for northward IMF, *J. Geophys. Res.*, *98*, 187, 1993*a*.

Song, P., C. T. Russell, and C. Y. Huang, Wave properties near the subsolar magnetopause: Pc 1 waves in the sheath transition layer, *J. Geophys. Res.*, *98*, 5907, 1993*b*.

Sonnerup, B. U. O., I. Papamastorakis, G. Paschmann, H. Luehr, Magnetopause properties from AMPTE/IRM observations of the convection electric field: Method development, *J. Geophys. Res.*, *92*, 12,137, 1987.

Southwood, D. J., and M. G. Kivelson, On the form of the flow in the magnetosheath, *J. Geophys. Res.*, *97*, 2873, 1992.

Takahashi, K., D. G. Sibeck, P. T. Newell, and H. E. Spence, ULF waves in the low-latitude boundary layer and their relationship to magnetospheric pulsations: A multisatellite observations, *J. Geophys. Res.*, *96*, 9503, 1991.

Traver, D. P., D. G. Mitchell, D. J. Williams, L. A. Frank, and C. Y. Huang, Two encounters with the flank low-latitude boundary layer: Further evidence for closed field topology and investigation of the internal structure, *J. Geophys. Res.*, *96*, 21,025, 1991.

Whipple, E. C., J. R. Hill, J. D. Nichols, Magnetopause structure and the question of particle accessibility, *J. Geophys. Res.*, *89*, 1508, 1984.

Williams, D. J., Magnetopause characteristics inferred from three-dimensional energetic particle distributions, *J. Geophys. Res.*, *84*, 101, 1979.

Williams, D. J., E. Keppler, T. A. Fritz, B. Wilken, and G. Wibberenz, The ISEE 1 and 2 medium energy particles experiment, *IEEE Trans. Geosci. Electron, GE-16*, 270, 1978.

Winske, D., S. P. Gary, D. S. Lemons, Diffusion transport at the magnetopause, in *Physics of Space Plasmas (1990)*, edited by T. S. Chang, G. B. Crew, and J. R. Jasperse, Scientific Publishers, Inc., Cambridge, Mass., 1991.

Zwan, B. J., and R. A. Wolf, Depletion of solar wind plasma near a planetary boundary, *J. Geophys. Res.*, *81*, 1636-1648, 1976.

R. R. Anderson, Department of Physics and Astronomy, University of Iowa, Iowa City, IA 52242.

R. J. Fitzenreiter, NASA Goddard Space Flight Center, Greenbelt, MD 20771.

S. A. Fuselier, Lockheed Palo Alto Research Laboratory, Palo Alto, CA 94304.

J. T. Gosling and M. F. Thomsen, Los Alamos National Laboratory, Los Alamos, NM 87545.

D. Hubert, Departement de Recherche Spatiale, Observatoire de Paris, Meudon, Meudon Principal Cedex, F-92195, France.

D. G. Mitchell, Applied Physics Laboratory, The Johns Hopkins University, Laurel, MD 20723.

G. K. Parks, University of Washington, Seattle, WA 98195.

C. T. Russell, Institute of Geophysics and Planetary Physics, University of California, Los Angeles, CA 90024.

P. Song, High Altitude Observatory, National Center for Atmospheric Research, P. O. Box 3000, Boulder, CO 80307.

(Received July 16, 1992;
revised February 25, 1993;
accepted March 1, 1993.)